RSC Advances

PAPER

View Article Online
View Journal | View Issue

Cite this: *RSC Adv.*, 2022, **12**, 13295

Development of antioxidant-rich edible active films and coatings incorporated with de-oiled ethanolic green algae extract: a candidate for prolonging the shelf life of fresh produce†

Kona Mondal, Sayan Kumar Bhattacharjee, Chethana Mudenur, Tabli Ghosh, Vaibhav V. Goud and Vimal Katiyar *

The concept of sustainability and the substitution of non-biodegradable packaging using biodegradable packaging has attracted gigantic interest. The objective of the present study was to revalorize the biowaste "de-oiled green algae biomass (DAB)" of *Dunaliella tertiolecta* using a green approach and the development of biodegradable chitosan (CS)-based edible active biocomposite films and coatings for prolonging the shelf life of fresh produce. Ultrasound-assisted green extraction was conducted using food-grade solvent ethanol for obtaining the bio-actives, namely "crude algae ethanolic extract (CAEE)" from DAB. The edible films (CS/CAEE) and coating solutions were developed by incorporating CAEE with varying concentrations (0 to 28%). The CAEE was subjected to MALDI-TOF-MS, NMR, and other biochemical analyses, and was found to be rich in DPPH antioxidant activity (~40%). The CS/CAEE films were fabricated using a solvent casting method and characterized by several biochemical and physicochemical (FESEM, TGA, FTIR, XRD, WVP, UTM, and rheological) characterization techniques. The addition of CAEE into the CS matrix reduced the maximum film transparency (~20%), water vapor permeability (~60%); improved the crystallinity (~24%), tensile strength (~25%), and antioxidant activity (~27%); and exhibited UV-Vis blocking properties as compared to the control film. Besides, the developed coating solutions and CAEE showed biocompatibility with BHK-21 fibroblast cells and antimicrobial activity against common food pathogens. The developed coating solution was applied on green chilli using a dipping method and stored at ambient temperature (25 ± 2 °C, 50–70 % RH) for 10 days. The shelf life of chillies was extended without altering the quality as compared to uncoated green chillies. Therefore, the formulated coating could be applicable for prolonging the shelf life of fresh produce.

Received 13th February 2022
Accepted 16th March 2022

DOI: 10.1039/d2ra00949h

rsc.li/rsc-advances

Introduction

Active and edible packaging is an emerging concept that aims to deliver quality and safe food along with a prolonged shelf life while at the same time mitigating environmental hazards caused by non-biodegradable food-packaging waste. Besides providing barrier properties, this innovative packaging also acts as a preservation method. The improved functionality of this packaging material is due to the incorporation of certain active substances, that are not available in conventional packaging.[1,2] In general, the active packaging system consists of antimicrobial agents, antioxidants, and several other beneficial compounds.[3] In recent times, a mass of the scientific community has focused their research predominantly on the development of biodegradable active edible packaging utilizing various natural bioresources as a functional preservative with due concern for food safety and security for consumers, overcoming the environmental drawbacks of current packaging, and the preservation of fossil fuel resources.[4,5]

In this context, chitosan, a biodegradable, nontoxic, bio-based substance with good film-forming properties and biocompatible polymers, obtained from the deacetylation of chitin, found in crustaceans and insects,[6] has received much attention for the development of active and edible food-packaging materials.[7] Chitosan is a linear polysaccharide, associated with the β-(1-4) glycosidic bond between D-glucosamine and *N*-acetyl-D-glucosamine (NADG). Interestingly, it is one of the potential candidates for developing active packaging materials among other polysaccharides due to its inherent antimicrobial and antioxidant activity based on its concentration and molecular weight.[2] Chitosan-based films and coatings

Department of Chemical Engineering, Indian Institute of Technology Guwahati (IITG), Assam-781039, India. E-mail: vkatiyar@iitg.ac.in

† Electronic supplementary information (ESI) available: Supporting figures and tables. See https://doi.org/10.1039/d2ra00949h

have demonstrated wide antimicrobial properties against Gram-positive, Gram-negative, yeast, and molds, due to the presence of certain cations that lead to surface damage in the microbial cell *via* interacting with the anions present in it.[8] Besides, chitosan can restore essential oils and bioactive compounds into their natural structure, which diversify its applications in controlled-drug delivery and food-coating systems.[9,10] Nevertheless, there has been a limited use of chitosan-based films in the area of food packaging to date due to its inherent poor barrier and mechanical properties, which makes it hydrophilic and brittle, which are undesirable properties for a food-packaging material where high strength, control of moisture, and gas transfer are essential.[11] To overcome these limitations biofillers, such as oil, lipids, fatty acids, waxes, proteins, polysaccharides, and various plant extracts, have been added to chitosan for obtaining improved physicochemical and structural properties.[12] However, the addition of oils and lipids adversely affect the mechanical properties of chitosan by altering the three-dimensional (3D) network structure.[13] Further, the incorporation of proteins and polysaccharides into chitosan films sometimes provide incompatibility for certain uses; thereby restricting their use. In this regard, Ferreira *et al.* (2009)[14] reported that whey protein-rich surfaces are more hydrophobic than chitosan; however, enhancing the protein amount decreased the mechanical strength and elongation. Furthermore, the concept of developing selected biopolymer-based multi-layered films and composites as biodegradable packaging materials has attracted a lot of attention due to the improved mechanical and other properties possible; albeit the higher cost limit the use of this concept.[15,16] In this context, a promising strategy has been put forward to address all the limitations and to prompt the development of novel sustainable packaging materials *via* utilizing the concept of green technology, where various biomaterials from different Agri-based waste may be utilized as a key factor for fabricating eco-friendly packaging materials.[17,18] In this regard, various plant-based extracts, such as banana peel extract,[19] pomegranate peel extract,[9] mutra leaf extract,[20] extract of pine nut shell, peanut shell, jujube leaf,[21] and others, have been used as biofillers in the chitosan matrix, and the associated literature on these have reported improvements in the antioxidant and other functional properties of the developed biocomposites. Recently, one study reported that the addition of spice extract into chitosan film enhanced different characteristic properties of the film and extended the shelf life of a food material.[22] Besides, Lorenzo *et al.* (2018) reported the non-toxicity of the plant extract at a higher dose level compared to doses taken through daily diets.[23]

Dunaliella tertiolecta is a green microalga that has been mostly studied for bio-energy production.[24] However, it also has potential use in the pharmaceutical and food industries as a healthy food supplement due to its bioactive compounds.[25] Predominantly, *Dunaliella* algae biomass has been utilized for biodiesel and bioethanol production.[26] Moreover, after extraction of the oil, the de-oiled residue or leftover part is recognized as de-oiled green algae biomass (DAB), which has commonly been treated as cattle feed or dumped in coastal regions, whereby it is responsible for causing negative environmental impacts. However, fresh algae biomass has gained much attention in various sectors compared to the residual part, with very few studies focused on de-oiled ABR. Interestingly, this waste is rich in several bioactive compounds, such as carbohydrates, proteins, and carotenoids.[27] In this context, Deshmukh *et al.* (2021) reported on the development of chitosan-based biocomposites for food packaging, whereby *Chlorella* de-fatted biomass powder was added as a biofiller material.[4] In addition, cellulose nanocrystals have been isolated from *Dunaliella* DAB and utilized as one of the potential biofillers for the development of poly(lactic acid)- and poly(ε-caprolactone)-based biodegradable biocomposites, as reported in our previous study.[28,29]

The present study focuses on the ultrasound-assisted green technology-based liquid extraction of bioactive compounds from *Dunaliella* DAB and the development of chitosan (CS)-based active edible biocomposite films and coatings. The ultrasound-assisted crude algae ethanolic extract (CAEE) was used in varying concentrations as a biofiller/food additive in the chitosan matrix to obtain active edible packaging materials with several improved physicochemical and functional properties. Further, the developed filmogenic solution was applied to a real food system as a primary packaging material in the form of an active edible coating, with an aim to extend the shelf life. Moreover, several physicochemical and functional properties of the developed films were studied. Further, the coating effects were confirmed by conducting physicochemical studies of coated green chilli. Interestingly, to the best of our knowledge, this is the first study on the development of an active edible food-packaging material additivated with *Dunaliella tertiolecta* green algae biomass extract. Further, more detailed experiments, analyses, and observations of the developed edible films and coating applications on various fresh produce have been documented elsewhere (Indian patent file no. 202131013653).

Experimental

Extraction of the de-oiled crude algae ethanolic extract

The green extraction of the de-oiled algae residue powder (provided by TERI, India) of *Dunaliella tertiolecta* is depicted in Fig. 1. Here, 50 gm of the standardized particles of the de-oiled algae biomass residue (passing through a 40 mesh sieve) was added into 500 mL ethanol (Finner, India) and kept under shaking overnight, before being subjected to ultrasound-assisted extraction. An ultrasonicator probe (Biologics, Inc., USA) was used for the extract preparation and sonication was conducted for 2–3 min, at room temperature, 20 kHz at 99% efficiency. Thereafter, the suspension was subjected to centrifugation at 5000 rpm for 5 min to separate the solid part from solution, and finally, filtration was conducted using Whatman filter paper no. 3 for obtaining the clear transparent green-colored crude algae ethanolic extract (CAEE) without any particles. Finally, the obtained extract was kept at −20 °C in the dark until further use.

Fabrication of biocomposites active edible films and coatings

The films were prepared by a solution casting technique, as described in Fig. 1. The concentrations of chitosan (CS, medium molecular weight, Sigma Aldrich, (USA)) (1 g/100 mL filmogenic solution) and acetic acid (Finner, India) (0.3%) were kept constant. Afterwards, the incorporation of CAEE to the CS solution was followed with varying the amount of CAEE at concentrations of 0, 4, 8, 12, 16, 20, 24, and 28 mg g^{-1} of CS. The solution was magnetically stirred for 24 h at room temperature. The developed filmogenic solution was kept under a vacuum drier for stabilizing the air bubbles generated from the solution for 2 h. Thereafter, the solution was spread over Teflon plates (140 cm dia) and dried at 40 °C for 24 h inside a hot air oven. A digital micrometer (Indi 6156, India) was used to measure the average film thickness by taking 10 random measurements on the film surface. Finally, the formulated filmogenic solution was applied as an active edible coating material (Fig. 1).

Characterization

Determination of the chlorophyll content of CAEE. The chlorophyll content of CAEE of the dried spent algae biomass was measured *via* UV-Vis spectrophotometry (PerkinElmer, USA) at wavelengths (λ) of 663 and 645 nm. The concentrations of total chlorophyll (Total Chl), chlorophyll a (Chl 'a'), and chlorophyll b (Chl 'b') were determined using the following equations:[64]

$$\text{Total Chl} = 8.02 \times A(663) + 20.2 \times A(645)$$

$$\text{Chl 'a'} = 12.7 \times A(663) - 2.69 \times A(645)$$

$$\text{Chl 'b'} = 22.9 \times A(645) - 4.68 \times A(663)$$

The yield of chlorophyll from the CAEE using the green solvent *via* ultrasonic extraction was calculated with the below equation:

$$\text{Yield } (\text{mg mL}^{-1}) = \left[\frac{\text{chlorophyll content}\left(\text{mg mL}^{-1}\right) \times \text{volume of the solvent (mL)}}{\text{weight of dried spent algae biomass (g)}}\right]$$

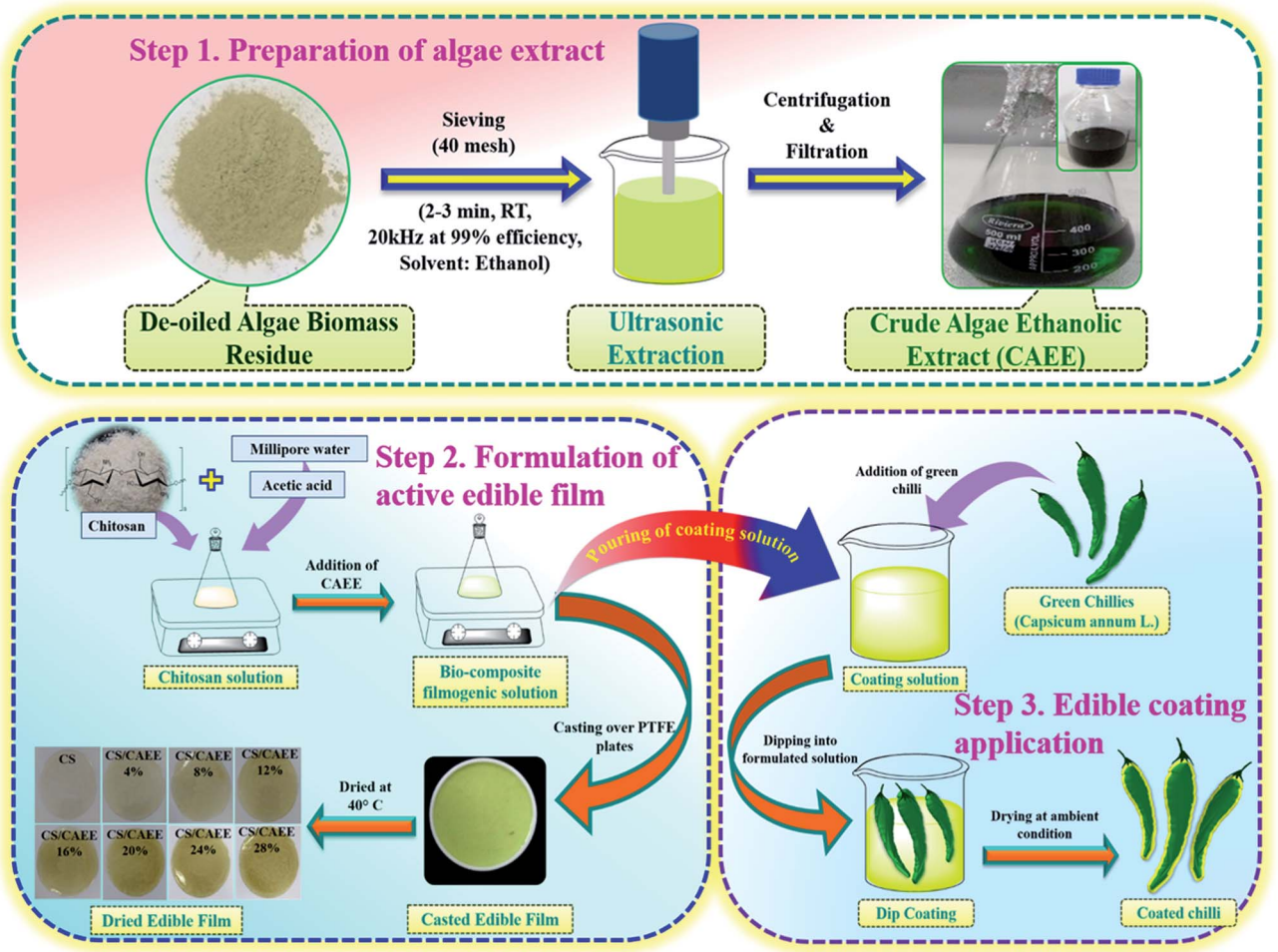

Fig. 1 Extraction of the biofiller CAEE and fabrication flowsheet of the active edible films and coating.

Nuclear magnetic resonance (NMR) analysis of CAEE. The proton (^{1}H) and carbon (^{13}C) NMR spectra of CAEE were recorded on a Bruker (ASCEND™ 600 MHz) NMR spectrometer attached with a TCI Cryo Probe. Concentrated extract of CAEE of ~70 mg was dissolved in two different solvents (0.7 mL) separately: deuterated chloroform ($CDCl_3$) and deuterated methanol (CD_3OD) containing the internal standard tetramethylsilane (TMS 0.03% (v/v)), respectively. After filtering with a PTFE (0.25 μm) micron filter, the solution was subjected to analysis. The ^{1}H and ^{13}C spectra were measured in the ppm range of 0 to 10 (32 scans) and 0 to 200 (900 scans), respectively.

Matrix-assisted laser desorption/ionization–time of flight (MALDI-TOF) mass spectroscopy analysis of CAEE. The CAEE was mixed with the matrix solvent 2,5-dihydroxybenzoic acid (DHB), prepared by dissolving in methanol (10 mg mL^{-1}) with 0.1% TFA. The sample was prepared at a ratio of 1 : 6 (matrix : CAEE), which meant 1 μL of matrix solution was added to 6 μL of analyte solution (CAEE). MALDI-TOF-MS analysis was performed on a Bruker Autoflex Speed spectrometer at an accelerating voltage of 19 kV (per spectrum around 2000 laser shots). The sample with the matrix solution was placed over a stainless-steel plate and dried before being subjected to the analysis. The spectrum reproducibility was checked by taking measurements at five different spots on the sample.

Determination of the antioxidant capacity. The free radical-scavenging properties of the CAEE and the developed CS-based biocomposites/active edible films were quantified using the DPPH (2,2 diphenyl-picrylhydrazyl, Aldrich, USA) free radical-scavenging activity method according to Dudonné *et al.* (2009), with slight modification.[65] In this study, ethanol was used as a reference instead of methanol. The DPPH solution was prepared by dissolving in ethanol (50 mg L^{-1}) and 3 mL of it was added to 1 mL of algae extract solution. Similarly, the film extract solution (1 mL) was mixed with 3 mL of DPPH solution and kept in the dark at room temperature for 30 min. Finally, the absorbance was measured at 517 nm. The percentage of DPPH free radical-scavenging activity was measured according to the following equation:

$$\text{DPPH scavenging activity}(\%) = \frac{\text{Abs}_{\text{DPPH}} - \text{Abs}_{\text{sample}}}{\text{Abs}_{\text{DPPH}}} \times 100$$

Determination of the total phenolic content. The total phenolic content (TPC) of CAEE were determined by the Folin–Ciocalteu (Himedia, India) method.[66] Here, a small quantity of extract (500 μL) was mixed with 2.5 mL of Folin reagent (distilled water : F–C reagent = 10 : 1), followed by the addition of 2 mL of sodium carbonate (Himedia, India) (7.5%, diluted in distilled water) into the mixture after 5 min. The absorbance of the solution was measured at 740 nm after an incubation period of 2 h in the dark. The result was determined using the standard gallic acid (Himedia, India) curve and reported in terms of μg of gallic acid per mL of extract.

Color parameters. The color coordinates of the CAEE and active edible films were determined using a colorimeter (Datacolor 550, Datacolor Technology Suzhou Co., Ltd., China) controlled by the Datacolor tools software program. The color values L^*, a^*, and b^* are indicators of lightness, and the degree of redness ($+a$) to greenness ($-a$), and yellowness ($+b$) to blueness ($-b$). The results for the CAEE and film samples were obtained in triplicate.

Transparency of the active edible films. The ultraviolet and visible-light barrier properties of the edible films were determined according to Fang *et al.* (2002), using a UV-Vis spectrophotometer (PerkinElmer, USA).[67] Film samples with the length and width of 10.0 cm and 1.5 cm, respectively, were placed in the cuvette for allowing the light beam to pass through the film surface. The film transparency was measured in the transmittance mode in the scan wavelength range between 200 and 800 nm.

Field-emission scanning electron microscopy (FESEM). The morphological behavior of the active edible films was investigated by FESEM (field-emission scanning electron microscopy, Sigma 300, Zeiss, Germany). Gold coating (SC7620, Quorum) was performed to make the sample conductive.

Thermogravimetric analysis (TGA). TGA analysis was performed to investigate the thermal behavior, including weight loss, maximum degradation, and gas absorption of the active edible film samples while heated at a constant heating rate under an inert atmosphere. This analysis was performed to check and compare the thermal stability of the films (~8 mg) using a thermogravimetric analyzer (TGA-4000, PerkinElmer, U.S.A.) under an inert nitrogen atmosphere at a flow rate of 50 mL min^{-1}. The samples were placed in the platinum crucible and heated from 30 °C to 700 °C at a heating rate of 10 °C min^{-1} under a nitrogen atmosphere.

Fourier-transform infrared spectroscopy (FTIR). The de-oiled algae biomass residue powder, CAEE, and film samples were analyzed by attenuated total reflection Fourier-transform infrared (ATR-FTIR) spectroscopy (Spectrum One, PerkinElmer, Inc., USA) to examine the change in functional groups during extraction. The obtained spectra were recorded in the range of 4000–500 cm^{-1}, with a resolution of 4 cm^{-1} and an accumulation of 16 scans.

X-ray diffraction (XRD). An X-ray diffractometer (Rigaku Smart Lab, Japan) was used to check the crystalline behavior of the active edible films, with CuK_α used as the radiation source to generate the X-rays. The wavelength (λ) of the incident X-ray was 1.54 Å. The Brag intensity was recorded within the 2θ range of 10–40° with a scan rate and sampling step angle of 20° min^{-1} and 0.02°, respectively. The percentage crystallinity index (I_{CR}) was determined using the following equation:

$$\%\ \text{crystallinity index}\ (I_{CR}) = \frac{\text{area of crystalline peaks}}{\text{area of crystalline peaks} + \text{area of amorphous peaks}} \times 100$$

Water vapor permeability (WVP). The water vapor permeability (WVP) of the active edible films was measured by a water vapor permeability tester (Mocon, PERMATRAN-W® 1/50G) as

per the ASTM E398 standard protocol. Samples were vacuum dried for 2 h at room temperature before the analysis. A 50 cm^2 area was exposed for the test at 37.8 ± 0.5 °C with a difference of 40% RH. Nitrogen gas (99.9% purity) was purged through the films during the analysis. The standard mode was selected to perform the test. After reaching the saturation point, the obtained water vapor transmission rate (WVTR) values were noted. The WVP of the film was calculated using the following equation:

$$\mathrm{WVP} = \frac{\mathrm{WVTR} \times L}{\Delta P}$$

where WVTR is the test result obtained from the instrument after completion of a cycle in (g m^{-2} day), L indicates the thickness of the film, and ΔP is the pressure difference at 37.8 °C saturated vapor pressure condition. The WVP is reported in this work in kg m m^{-2} Pa^{-1} s^{-1}. All the tests were performed in triplicate.

Mechanical properties. According to ASTM D-882, the tensile strength (MPa) and elongation at break (%) of developed films were determined using a universal testing machine (Zwick/Roell Z005). Samples were prepared by cutting the film into rectangular bars (10 mm × 50 mm) and then fixing them within the machine with a grip separation of 20 mm. The test speed was 5 mm min^{-1}, which was obtained using a cell load of 5 kN. The reported data were obtained from experiments performed in triplicate.

Rheological properties. The rheological measurement of steady-state flow and dynamic viscoelasticity was conducted in a controlled stress rheometer (Anton Parr) with a cone and plate geometry (angle < 4°, diameter = 50 mm, gap = 0.215 mm). The measurement was carried out at room temperature, maintained by the Peltier system temperature controller. All the measurements were performed in triplicates.

Steady shear measurements. Steady shear experiments or the flow curves of the solutions were carried out at room temperature (25 °C) by varying the viscosity of the solutions as a function of the shear rate (0.1–1000 s^{-1}). Experimental data were fitted to the Ostwald–de Waele model or power-law model to determine the Newtonian or pseudoplastic behavior of the solutions through the following equation:

$$\eta = m(\dot{\gamma})^{n-1}$$

where 'm' and 'n' are the fluid consistency coefficient and the flow behavior index, respectively.

Strain sweep measurements. Strain sweep measurements of the solutions were done to determine the linear viscoelastic region (LVER) by varying the strain amplitude at a fixed frequency value of 1.0 Hz at room temperature (25 °C), with the storage modulus, G', and the loss modulus, G'', kept constant.

Different rheological parameters were analyzed:

- G'_{LVER}, the storage modulus at the critical strain.
- γ_{L}, the critical strain.
- tan δ, the ratio of loss to the storage modulus, which determines the liquid or solid behavior of the solutions.
- The difference between the moduli G''–G' at a fixed strain value, which depicts the reinforcing effect of the extract incorporation of the solutions in their viscous and elastic behaviors.

Frequency sweep measurements. Dynamic frequency sweep measurements were performed at room temperature (25 °C) by varying the frequency in a range of 0.1–100 rad s^{-1} with a fixed strain value of 1% (in the LVER), which was determined from the amplitude sweep analysis. This allows determining the behavior of the elastic and loss moduli with the increase in the frequency and with the incorporation of the extract.

Antimicrobial activity. The two most common food pathogens, namely Gram-negative *Escherichia coli* and Gram-positive *Staphylococcus aureus*, were used for the analysis of the antibacterial activity of neat chitosan (nCS) and CAEE-incorporated formulated CS-based filmogenic/coating solutions. A freshly prepared bacterial culture suspension of about 100 μL was spread over Luria–Bertani agar culture medium. The filter paper was cut using a paper cutter punching machine, manually followed by dipping into each biocomposite/filmogenic coating solution before placing it over the plate surfaces and incubating at 37 °C for 24 h.[41] The appearance of a clear inhibition zone diameter was recorded.

Cytotoxicity study

Seeding and culturing of the cells. Dulbecco's modified eagle's medium (DMEM) (Gibco™) was used to culture BHK-21 (Baby Hamster Kidney Fibroblast) cells (at passage-42). Fetal bovine serum (FBS) (10%) and an antibiotic–antimycotic cocktail (1%) were also added to the DMEM and the culture medium along with the cells and maintained at 37 °C in a humidified atmosphere with 5% CO_2. After staining with trypan blue stain (SRL), the cells were counted by the Countess® II FL Automated Cell Counter (Thermo Fisher Scientific). One day before, the cells were seeded (100 μl per well) in five 96-well plates.

MTT assay. The mitochondrial activity of BHK-21 cells seeded onto the biocomposite filmogenic/coating solutions was assessed by the enzymatic conversion of tetrazolium dye MTT 3-(4,5-dimethylthiazol-2-yl)-2,5-diphenyltetrazoliumbromid after the time intervals of 8, 16, 24, 48, or 72 h. The samples were prepared from 10% (v/v) concentration in plain DMEM (standard culture media without serum), in which plain DMEM was used as a control. Next, 100 μL of each sample and control was added to all the plates in four replicates after removing the seeding media (standard culture media) followed by incubation at 37 °C under a humidified atmosphere with 5% CO_2 for different time intervals (8, 16, 24,48, 72 h). Meanwhile, MTT stock solution of 5 mg mL^{-1} was prepared in PBS and stored at 4 °C. After the incubation periods of the respective plates, all the samples were removed and 100 μL of MTT solution diluted in plain DMEM to 0.5 mg mL^{-1} was added, followed by incubation at 37 °C in a humidified atmosphere with 5% CO_2 for 3 h. Afterward, the MTT solution was discarded and 100 μL of DMSO was added to each well and the plates were incubated at 37 °C in a humidified atmosphere with 5% CO_2 for 10 min to dissolve the formazan crystals. Cell viability was determined by taking the absorbance at 570 nm using a 96-well plate reader (Thermo

Fischer Scientific). Graphs were plotted using the closest absorbance values of three replicates out of the four replicates of each sample.

Shelf-life study of green chilli (*Capsicum annum* L.)

Edible coating on green chilli. Green chillies (*Capsicum annum* L.) were procured from the local market of IIT Guwahati. The samples were washed with lukewarm water and 0.2% sodium hypochlorite solution for removal of any extraneous matter, like dirt, mud, *etc.* After sorting and washing the samples, they were subjected to air-drying for 2 h at room temperature. A simple easy dip-coating technique was selected to coat the samples according to the method represented in Fig. 1. Each chilli was dipped into a beaker containing coating the solution for 1 min duration and this step was repeated three times at intervals of 3 min. After the coating, the samples were stored under ambient conditions (25 ± 2 °C, 50–70 % RH).

Physiological parameters of the coated green chilli

Weight loss. Weight loss and surface shriveling are the two most important properties that need to be controlled after harvesting fresh produce. The weight loss of the green chillies during the storage days was measured by taking the weight of each sample at a specific time interval. The results were expressed as a percentage weight loss. Further, weight loss is an indication of respiration occurring in post-harvest fruits and vegetables.[68] The weight loss was calculated using the following equation:

$$\text{Weight loss } (\%) = \frac{\text{initial weight} - \text{final weight}}{\text{initial weight}} \times 100$$

Microstructure and color parameters of the stored chili. The surface of the coated samples along with uncoated was visualized under an optical polarized microscope for observing the changes on the green chilli surface before and after coating. The color parameters lightness (L^*) and chromaticity (a^* and b^*) of the stored chillies were determined using a colorimeter (DATACOLOR 880, USA). The results were reported obtained after taking three measurements on the sample surface from each of five sets of samples in a single batch.

Firmness. A texture analyzer (TA.XT plus, Stable Microsystems, UK) was used to measure the firmness of the stored fruits with the help of Texture Expert software (Version 1.22; Stable Microsystems, UK). The load cell used for the measurement was 5 kg. The Warner–Bratzler Blade was used to determine the firmness by intersecting the chillies at different areas with the test speed of 0.5 mm s^{-1} and with an automatic return. The pre-test and post-test speeds were set at 2 mm s^{-1}.

Statistical analysis. Analysis of variance (ANOVA) was performed on the data sets using SPSS 26.0 software and significant effects ($p < 0.05$) were noted. Significant difference among the means was determined by Tukey's Test.

Results and discussion

Biochemical analysis of the biofiller CAEE

The ultrasound-assisted extraction from de-oiled algae biomass residue is schematically described in Fig. 1. The CAEE was rich in antioxidants with 40 ± 1.41% DPPH radical-scavenging activity, a total phenolic content of 515.72 ± 4.67 μg g^{-1}, total flavonoid content of 151.75 ± 2.05%, and total chlorophyll content of 23.81 ± 1.1 mg mL^{-1}, respectively. The yield of chlorophyll was 238.14 mg mL^{-1}, which indicated ethanol acted as a superior chlorophyll extracting solvent.[30] In addition, the CAEE contained a higher percentage of chlorophyll '*a*' (15.63 ± 0.16) compared to chlorophyll '*b*' (8.19 ± 0.09). Moreover, the obtained results indicated that the CAEE was rich in antioxidants and polyphenols. The color coordinates L, and a^* and b^* values of CAEE were 72.62 ± 0.04, −14.1 ± 0.01, and 59.29 ± 0.05, respectively. The negative value of a^* was attributed to the green color of the extract, which was due to the presence of the pigment chlorophyll, whereas the higher positive value of b^* indicated a yellow color, which could be due to the presence of carotenoids, such as β-carotene and others, which is the most available pigment found in green algae.[31]

MALDI-TOF-MS analysis of CAEE

Matrix-assisted laser desorption/ionization mass spectroscopy is one of the methods for the structural identification of organic matter of any biological sample. A series of masses m/z of CAEE were observed from the MALDI-TOF-MS spectrum and are depicted in Fig. 2. The obtained peaks at the lower m/z range of 89.22, 105.32, 117.25, and 181.42 corresponded to proteins alanine, serine, valine, and tyrosine, respectively.[32] Besides, the masses m/z at 183.98, 211.66, 232.74, 253.82, 258.21, 284.25, 324.94, 340.89, 344.73, 359.21, 372.41, 409.25, and 425.01 corresponded to protonated hexose sugar, sulfated hexose sugar, magnesium ion (Mg^+) attached with a hexose sugar, uronic acid, two hexose sugar, two pentose sugar with a Mg^+ ion, disaccharide (heptose and pentose), deprotonated di-saccharide

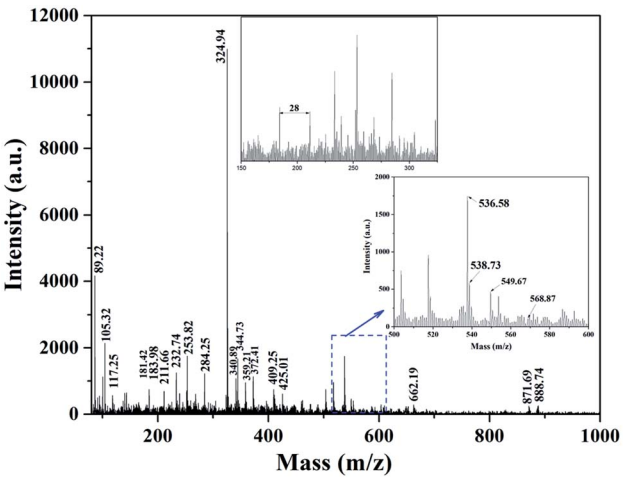

Fig. 2 MALDI-TOF-MS spectra of crude algae ethanolic extract (CAEE).

(hexose and heptose) associated with a sodium ion, and sugars linked with other ions, like Na, Mg, P, S, *etc.* The mentioned metals present in the de-oiled algae biomass were also detected by ICPMS analysis, as reported in our previous study.[28] The observed peak at *m*/*z* 662.19 might be related to the tetrasaccharide of two sugars, *i.e.*, both pentose and hexose. The mass deltas between the peaks were observed consecutively at 1–2, 14, 18, and 28 Da, corresponding to the degrees of saturation and ring structures, polymeric chains ($(CH_2)_n$), loss of water molecule and deprived CO bond from the esters of lactone.[32] Further, the *m*/*z* values in the range between 500 to 600 were predominantly responsible for the carotenoids. The MALDI spectra were highlighted and intensified for masses *m*/*z* at 536.58, 538.73, 549.67, 568.57, and 593.86, representing the presence of carotenoids, such as β-carotene along with its derivatives, zeaxanthin and deprotonated astaxanthin, which is similar to the reported literature by Fraser *et al.* (2007).[33] The identified peaks at *m*/*z* 871.69 and 888.74 corresponded to chlorophyll a or pheophytin and astaxanthin esters.[33]

Nuclear magnetic resonance (NMR) analysis of CAEE

^{1}H NMR. The proton (^{1}H) NMR spectra of the obtained algal extract (CAEE) of *Dunaliella tertiolecta* in the two different solvents, namely chloroform ($CDCl_3$) and methanol (CD_3OD), showed several peaks in the spectrum possibly due to the presence of various compounds and their derivatives, including exopolysaccharide, carotenoids, and proteins (Fig. 3a and SI†). The spectrum indicated the chemical shifts (ppm) and corresponding functional groups. Both the spectra predicted the presence of the α, β-anomeric carbon of hexose or pentose based on the chemical shift at 5.1 to 5.4 and between 4.8 to 4.9 ppm, respectively. The ppm value at 2.3 was attributed to the presence of uronic acid, which was also found in the MALDI-TOF-MS spectrum.[34] The presence of halide and N–H groups was attributed to the peaks at 3.0 ppm and 1.3 ppm. Further, the chemical shifts at 2.0 and 2.8 ppm were attributed to the functional groups related to the acetyl amine of hexose or pentose sugar moiety.[34] Moreover, along with polysaccharides, other functional groups attributed to the alkene, alkyne, aliphatic, aldehyde, and aromatic compounds could be found in the spectra, which can be more clearly seen in the magnified graphs (Fig. 3a and SI†). It is well known that *Dunaliella* species can accumulate quite a good quantity of pigments, mainly chlorophylls and carotenoids.[31] Among the chlorophylls, chlorophyll a was predominant, whereas β-carotene, astaxanthin, and fucoxanthin were mostly found in this species. The signals between 6–6.9, 2.0, 1.5, and 1.0 ppm were attributed to polyene $(CH{=}C{-}CH_3)_n$, vinyl CH_3, CH_2, and iso dimethyl attached to a cyclic ring, respectively.[25] In this context, the presence of β-carotene and astaxanthin pigments was also confirmed due to these signals. The observed chemical shift at 7.13 ppm in the doublet form in both the NMR spectra was related to the olefinic protons of fucoxanthin.[31] Further, the ^{1}H NMR spectra predicted the presence of proteins, such as alanine and tyrosine, in CAEE due to the appearance of chemical shifts at 3.62, 1.47, 2.30, 2.34, and 7.14. This finding corroborated the obtained mass results from the MALDI-TOF-MS spectrum. In this context, a similar observation was reported by Iglesias *et al.* (2019).[31]

^{13}C NMR. The ^{13}C NMR analysis of CAEE was carried out to confirm the presence of carotenoids, polysaccharides, and proteins and the absence of intensified saturated and unsaturated fatty acids. As can be conferred from Fig. 3b and SI,† none of the intensified peaks was found in the range of 170 to 175 ppm in both the spectra of the CAEE dissolved in $CDCl_3$ (Fig. 3b) and CD_3OD (SI†), which mainly corresponded to saturated carbonyl carbons, oleyl, linoleyl, alpha-linolenic acid, and acyl chains.[31] This result indicated the absence of saturated and unsaturated fatty acids, which are commonly found in algae. The occurrence of this result was expected as de-oiled algal biomass was utilized in the present study. The presence of peaks between 120 to 140 ppm corresponded to C11, C7, C5, C15, C10, C14, C12, and C8 carotenoids.[35] Further, the presence of olefinic groups was also confirmed by the observed peaks in the range from 127–132 ppm.[31] The presence of carbohydrates was assigned to the peak range from 60 to 106 ppm, whereas

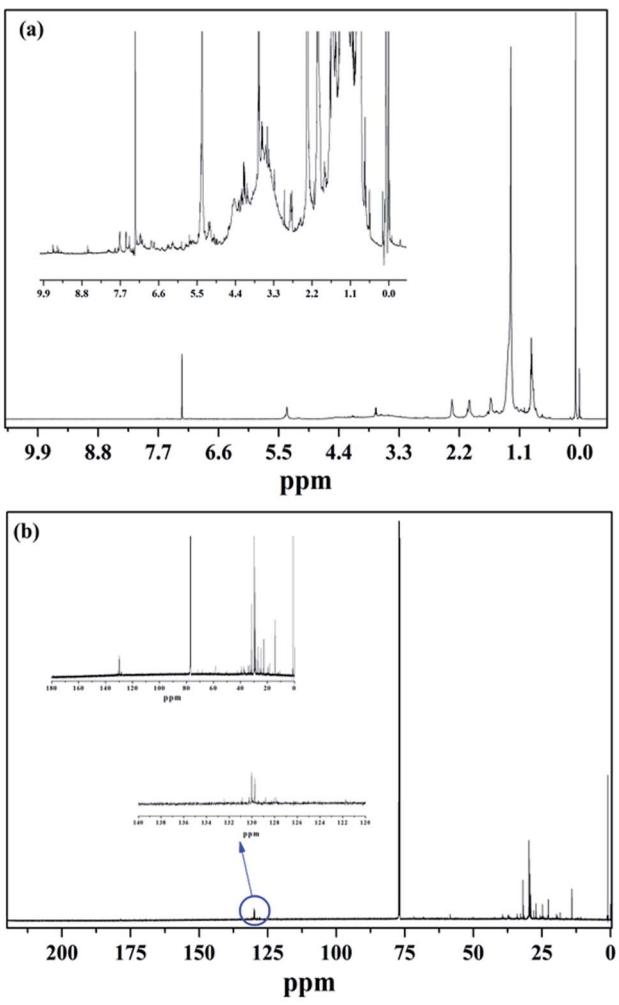

Fig. 3 (a) ^{1}H NMR spectra of CAEE in $CDCl_3$ solvent (b) ^{13}C NMR spectra of CAEE in $CDCl_3$ solvent.

proteins, like alanine and tyrosine, corresponded to the carboxylic group peaks found at 178.3, 58.5, 16.9, 59.5, 122.3, and 131.0 ppm. The presence of aromatic, amine, and sulfonic groups was identified in the spectra as shown in the ESI.† The presence of aromatic compounds was also noted following the results supported by the ^{1}H NMR analysis. Further, the NMR analysis results corroborated the MALDI-TOF findings.

Film characterization

Visual aspect and color parameters. The CS-based films presented homogeneity and an absence of insoluble particles regardless of the CAEE concentration, as shown in Fig. 1. The color parameter values (Table SI†) corroborated the differences in the visually observed yellow color intensity in the biocomposite films. In general, the L^* and a^* values decreased and b^* values increased as a function of increasing CAEE concentration (Fig. 4a and b), where L^*, a^*, and b^* correspond to the lightness, green, and yellow color, respectively. However, in this study, a negative a^* value was observed, which was attributed to the presence of chlorophyll pigments. The increment in negative a^* value with increasing the CAEE concentration was observed, with a maximum at 12% CAEE concentration, followed by a reduction until finally a positive value was obtained with the highest biofiller loading (Fig. 4b). The increment in negative a^* values might have been caused by the increasing concentration of chlorophyll or carotenoids in the higher CAEE loaded biocomposites, which is similar to the visual observation of biocomposite films. The positive a^* value might have been due to the occurrence of carotenoid derivatives during the drying of the film. In this regard, the reported literature says active films containing natural-colored pigments could be responsible for changing the values of the color coordinates. Wang *et al.* (2013) reported a reduction in L^* value and an increment in a^* and b^* values in a CS-based film after the incorporation of tea polyphenols as compared to a control film.[36]

Transparency of the film. The transparency of a film describes its optical nature and is another important parameter for food packaging. This is especially important since food is a complex system and many foods are sensitive toward light, *i.e.*, UV-Vis (ultraviolet-visible). It can be conferred from Fig. 4c that the neat CS (nCS/control) film presented higher transparency as compared to the biocomposites. The incorporation of CAEE into the CS matrix improved the barrier of light transmission to the visible and ultraviolet (<400 nm) regions. The addition of the extracts in the films reduced the transmittance values in the UV and visible-light region (400–800 nm), with a significant reduction in these values for visible light around 650 nm, whereas no blocking properties were found in the nCS film. Interestingly, an improvement in the blocking property was observed with increasing the biofiller concentration. In this regard, the presence of phenolic compounds in CAEE could provide UV-Vis blocking properties to the edible active films.[37]

Thermal stability of the films. The thermogravimetric (TGA) and derivative (DTG) thermograms of the control and biocomposite films are presented in Fig. 5a and b.

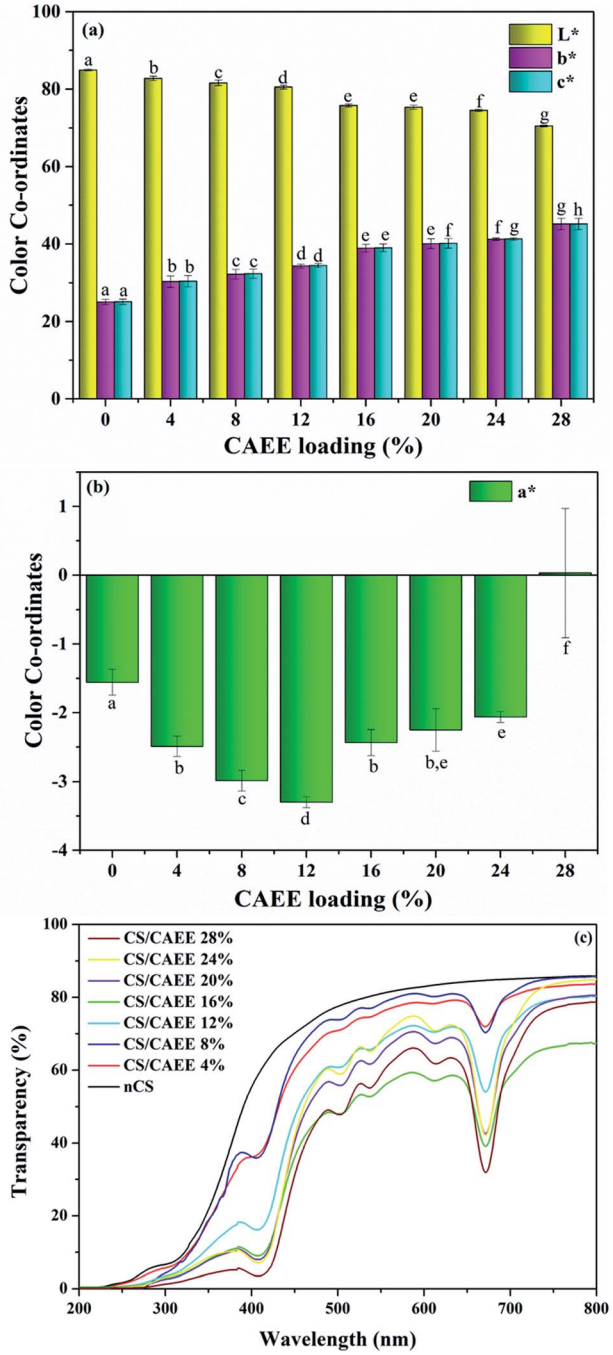

Fig. 4 Color coordinate values of (a) L^*, b^*, and c^* (b) a^*, and (c) UV-Vis light transparency of the CAEE incorporated edible active films (biocomposites) along with the control film.

A two-step degradation was recorded in each of the samples (Table SI†). The first stage of degradation was recorded around 50–100 °C (about 5% decomposition for each film), which could be attributed to the loosely bound water evaporation from the polymeric structures. The second step of degradation was observed between 270–320 °C and it could correspond to the decomposition of CS molecules and CAEE.[19] The predominant mass loss was recorded in the second degradation stage at

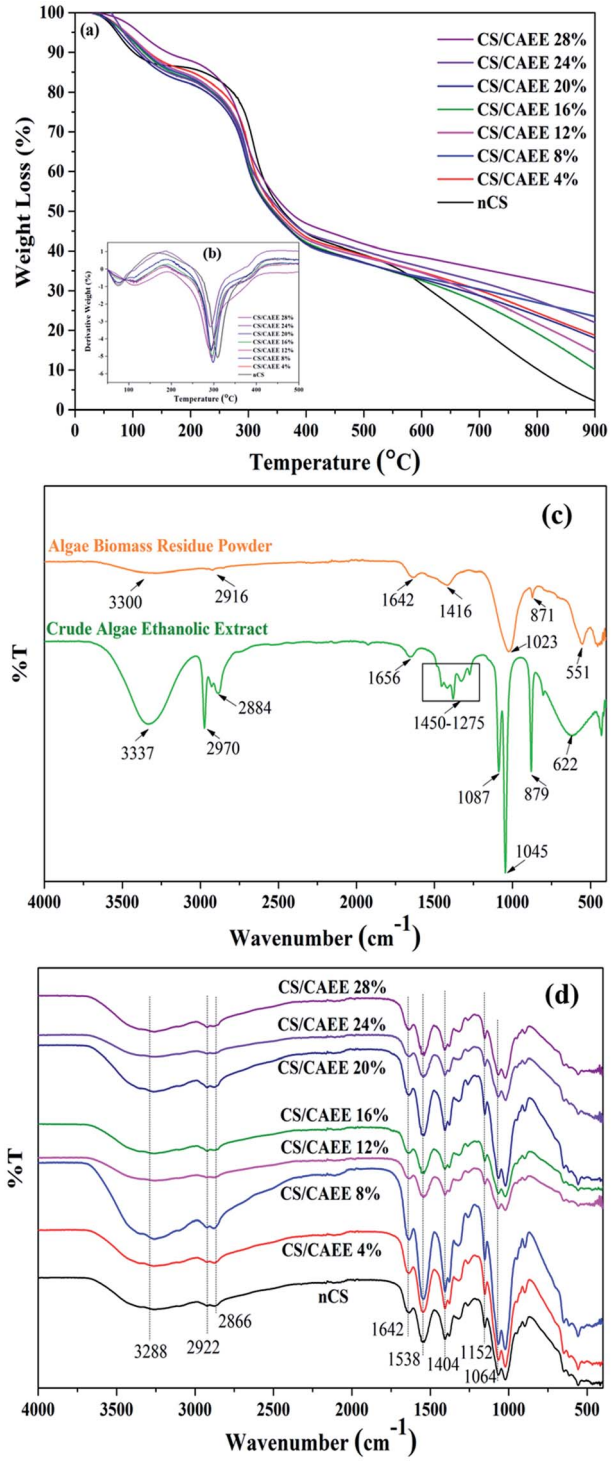

Fig. 5 (a) Thermogravimetric, and (b) derivative thermogram of CAEE incorporated edible active films (bio-composites) along with control film, (c) FTIR spectrum of de-oil algae residue powder and CAEE, and (d) FTIR spectrum of developed bio-composite films with control.

around 270–305 °C and it was because of the denaturation of the CS-polymeric organization and biofiller. In the second stage, the biocomposite films showed a slight reduction in mass loss as compared with the nCS film, which could be due to the formation of strong and heavy interactions *via* hydrogen bonding between CS molecules with the phenolic compounds of CAEE.[19] The temperatures at 5% ($T_{5\%}$) and 10% ($T_{10\%}$) mass loss are reported in Table SI,† where it can be seen that the biocomposite showed higher temperatures compared to the nCS film in both cases. Furthermore, the maximum temperature of the first degradation for the control film was ~75.5 °C (Table SI†) whereas, the incorporation of CAEE increased the temperature to 106.8 °C and 113.8 °C in the biocomposites, which indicated an improved thermal stability of the biocomposites compared to the nCS film. Similar types of observation have been reported previously, where the incorporation of sweet potato extract, banana peel extract, and others tailored the thermal stability in developed biocomposites.[19,38]

FTIR analysis. FTIR analysis of the de-oiled algae biomass residue powder (Fig. 5c) depicted the functional groups present on the surface of the residual *Dunalliela* biomass. The observed broadband ~3300 cm^{-1} belonged to –NH and –OH groups.[39] The frequency band at ~2916 cm^{-1} was attributed to –CH stretching. The bands at 1643 and 1416 cm^{-1} corresponded to the carbonyl (C=O) group and –C=S group the stretching vibrational.[40] The other lower region peaks were assigned to C–N and –C=S groups. The FTIR spectrum of CAEE (Fig. 5c) exhibited a broad absorption peak at ~3337 cm^{-1} attributed to –OH stretching. However, the observed absorption bands in the de-oiled algae biomass residue powder and the extract were different. A strong absorption peak was observed at 2970 cm^{-1}, corresponding to C–H symmetric stretching vibrations of the polyphenols. The presence of bands at 2884 and 1656 cm^{-1} might be attributed to ethanol and amide I, or C=O stretching of proteins or carboxylic acid, respectively. The presence of bands at 1276, 1327, and 1380 cm^{-1} could be related to CH_2 vibration, amide III, and symmetric CH_3(CO) vibration of 1,8-cineole, respectively. Further, the possibility of the presence of polysaccharides could be attributed to the occurrence of bands at 1087 and 1045 cm^{-1}. The observed band at 879 cm^{-1} corresponded to the $-CH_2$ stretching vibration of 1,8-cineole or ethanol. Fig. 5d depicts the spectra for the nCS and developed biocomposite edible films. The nCS displayed a wide absorption peak centered at 3288 cm^{-1}, which could be associated with stretching vibrations of N–H and O–H. The occurrence of peaks at 2922 and 1642 cm^{-1} might be attributed to C–H asymmetric stretching due to methylene groups and the C=O stretching vibration of the residual amide bond. The absorption bands at 1538 and 1404 cm^{-1} corresponded to amide II and amide III, while the peak at 1152 cm^{-1} was attributed to C–H and 1064 cm^{-1} was ascribed to C–O stretching vibration.[41]Moreover, while the incorporation of CAEE into the CS matrix exhibited variations in intensity, the frequency was unalerted.

Possible mechanism of the developed CS/CAEE film. The probable mechanism of the fabricated CAEE-incorporated CS-based biocomposite films is depicted in Fig. 6a. One of the potential candidates for developing edible films or biocomposites is CS due to its biocompatible, adequate film-forming property, high molecular weight, and charge density. The presence of amino (NH_2) and hydroxyl (OH) groups in the CS chain play a major role in the development of biocomposites

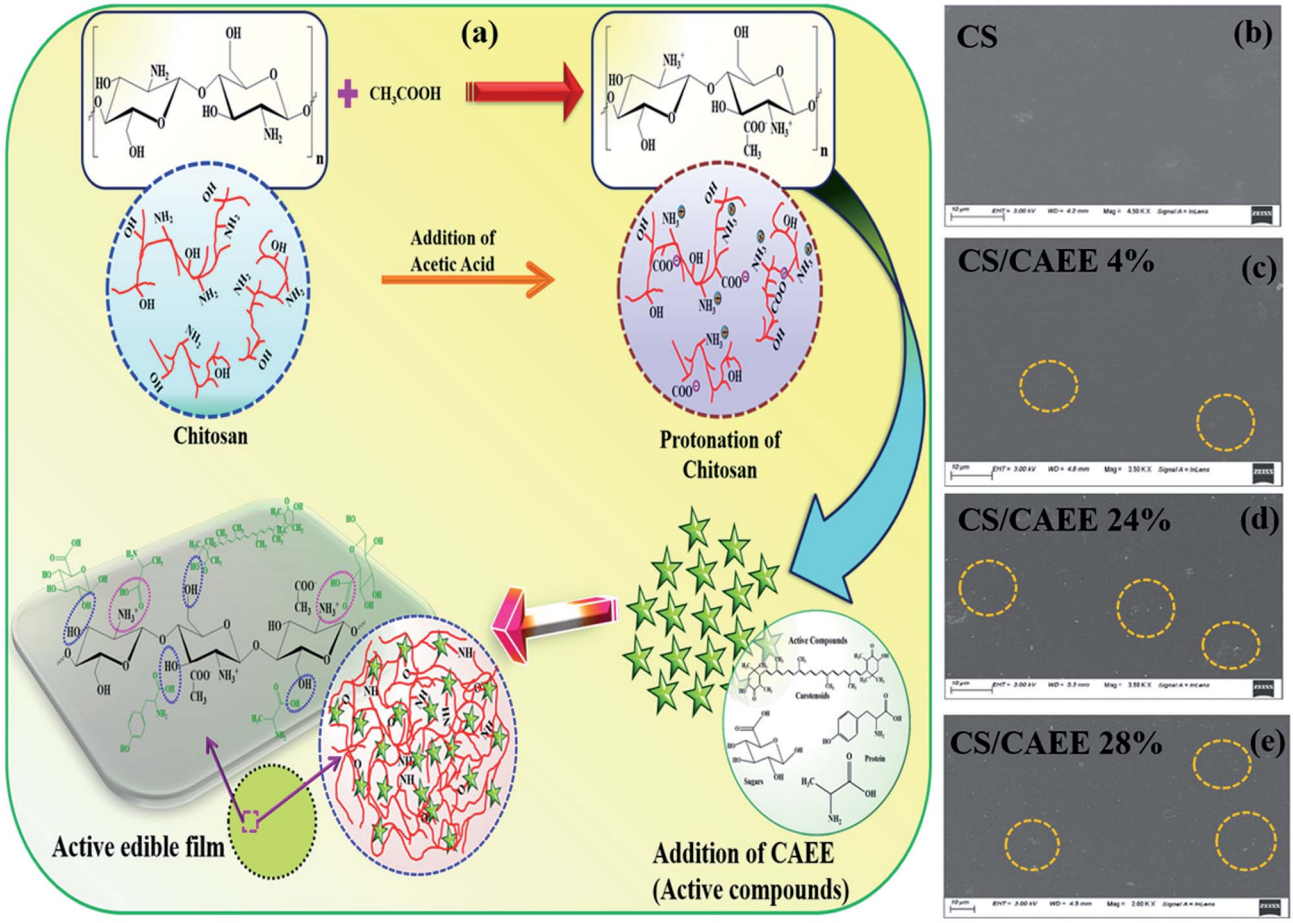

Fig. 6 (a) Probable mechanism of the CS/CAEE biocomposite film formation, and (b–e) surface morphology of the developed biocomposite films compared with the control.

via hydrogen, covalent, and amide bonding. The addition of mild acetic acid is required to dissolve CS, and CS then becomes protonated due to the occurrence of a cationic amine group (NH_3^+). As a result, the electrostatic repulsion within the CS molecules is reduced due to the protonation, which enhances the binding affinity with the added biofiller CAEE.[19] Further, CAEE contains an adequate number of bioactive molecules of polyphenols, such as carotenoids, proteins, polysaccharides, and sugars. These active molecules are strongly attached to the protonated chitosan chain *via* hydrogen bonding (dotted by the blue circle in Fig. 6a) and amide bonding (marked as the dotted magenta circle in Fig. 6a) as demonstrated in Fig. 6a and form the grafting between the active molecules and polymer matrix. The amide bonding majorly occurs between the protein molecules and cationic CS chains as proteins contain carboxylic group in their structure, which are highly attracted toward cationic amine groups, thereby a strong interaction occurs. In this context, Deshmukh *et al.* (2021) reported a strong interaction between the filler and the CS matrix when the *Chlorella* biomass was added *via* a bridging and patching phenomenon.[4] The formation of grafting by intermolecular interactions and encapsulation was reported while active compounds were incorporated into the pectin matrix.[18]

Film surface morphology. The surface characteristics of the nCS and CS/CAEE biocomposite films are presented in Fig. 6b–e. As can be seen from Fig. 6b, a smooth, compact surface morphology without the presence of cracks or pores was observed for the control, which concurred with the visual observation results. Nevertheless, the addition of CAEE in the biocomposite films exhibited irregular surfaces. The CS/CAEE film showed many tiny particles on the surface (Fig. 6c–e). The fabricated films exhibited heterogeneous surface roughness, which increased with the addition of a greater CAEE concentration. Small particles were observed in the biocomposites, whereas a greater number of particles was detected in the highest loading of 28% CAEE (Fig. 6e). It could be speculated that the bridging phenomenon occurred inside the biocomposites, whereby CAEE molecules partly bonded with CS chains while the rest of the CAEE molecules were attached to another CS chain.[4] The increased roughness was due to the occurrence of a higher number of bioactive molecules, including polyphenols, proteins, sugars, amino, acids, and polysaccharides. Almost similar surface morphologies were revealed after the addition of algae biomass and seaweed, as seen from the SEM micrographs in other reported works of CS-based and gelatin-based composite films.[4,42] Further, polarized

optical microscopic (POM) images of nCS and the biocomposites (SI†) agreed with the morphological behavior obtained from the FESEM images. The presence of nontoxic minerals, such as sodium, magnesium, calcium, potassium, and sulfur, along with oxygen, nitrogen, and carbon was found by energy-dispersive X-ray spectroscopy (EDX) analysis of the biocomposites (SI†). In this context, the presence of the aforementioned elements arose from the organic sources of CAEE containing polysaccharides, carotenoids, proteins, and sugars. Moreover, a homogeneous distribution of particles was observed in the biocomposites.

XRD analysis. Fig. 7a depicts the X-ray diffraction pattern of the nCS and developed biocomposite films. The characteristic peaks were observed at 9.69° and 20.54°, corresponding to the [020] and [110] planes, respectively. An increasing trend of crystallinity was observed after the addition of CAEE. A maximum improvement of ~22% crystallinity was obtained in the highest loading of CAEE (I_{CR} = 64%) compared to the nCS film (I_{CR} = 42%). The enhancement in the percentage of the crystalline index might be due to the strong intermolecular hydrogen bonding between the biofiller (CAEE) and polymer matrix (CS). Further, peak shifting was not observed in any of the sample XRD patterns, thereby indicating that no structural changes occurred after the addition of the biofiller with varying loading.

Water vapor permeability of the developed films. Fig. 7b depicts the water vapor permeability (WVP) of the developed edible biocomposite films and the effectiveness of the CAEE addition. A significant reduction was observed in the WVP values in the biocomposites due to the addition of CAEE. Further, the reduction was found to be highest with increasing the CAEE concentration from 4 to 28%. The highest reduction of ~60% was obtained in the biocomposite films with a 28% addition of CAEE compared to the control film. Moreover, the improvement in the WVP might be due to the strong intermolecular hydrogen bonding between the CS matrix and biofiller (CAEE), which probably allowed the formation of crosslinking, due to which the reduction in free space occurred inside the polymer matrix as a result of the lowered rate of diffusion of water vapor molecules through the biocomposite edible films. These observed findings were in also in line with the results of the improved crystallinity of the biocomposites, as revealed by the XRD analysis. Further, before the analysis, the films were dried at 100 °C for 2 h, and this particular step could have had

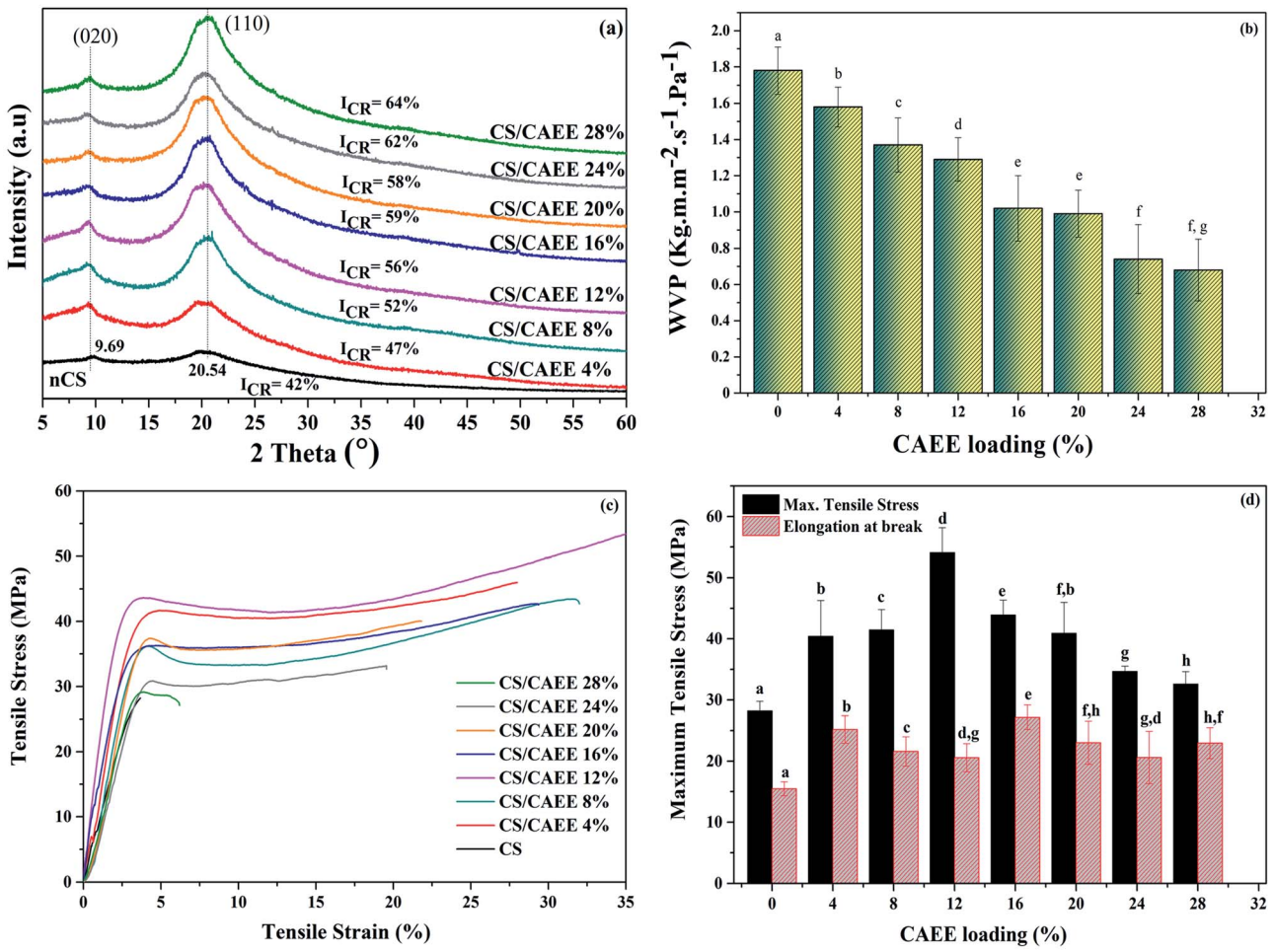

Fig. 7 (a) XRD patterns, (b) water vapor permeability results, (c) stress–strain curves, and (d) maximum tensile stresses and elongations at break of the developed biocomposite films compared with the control.

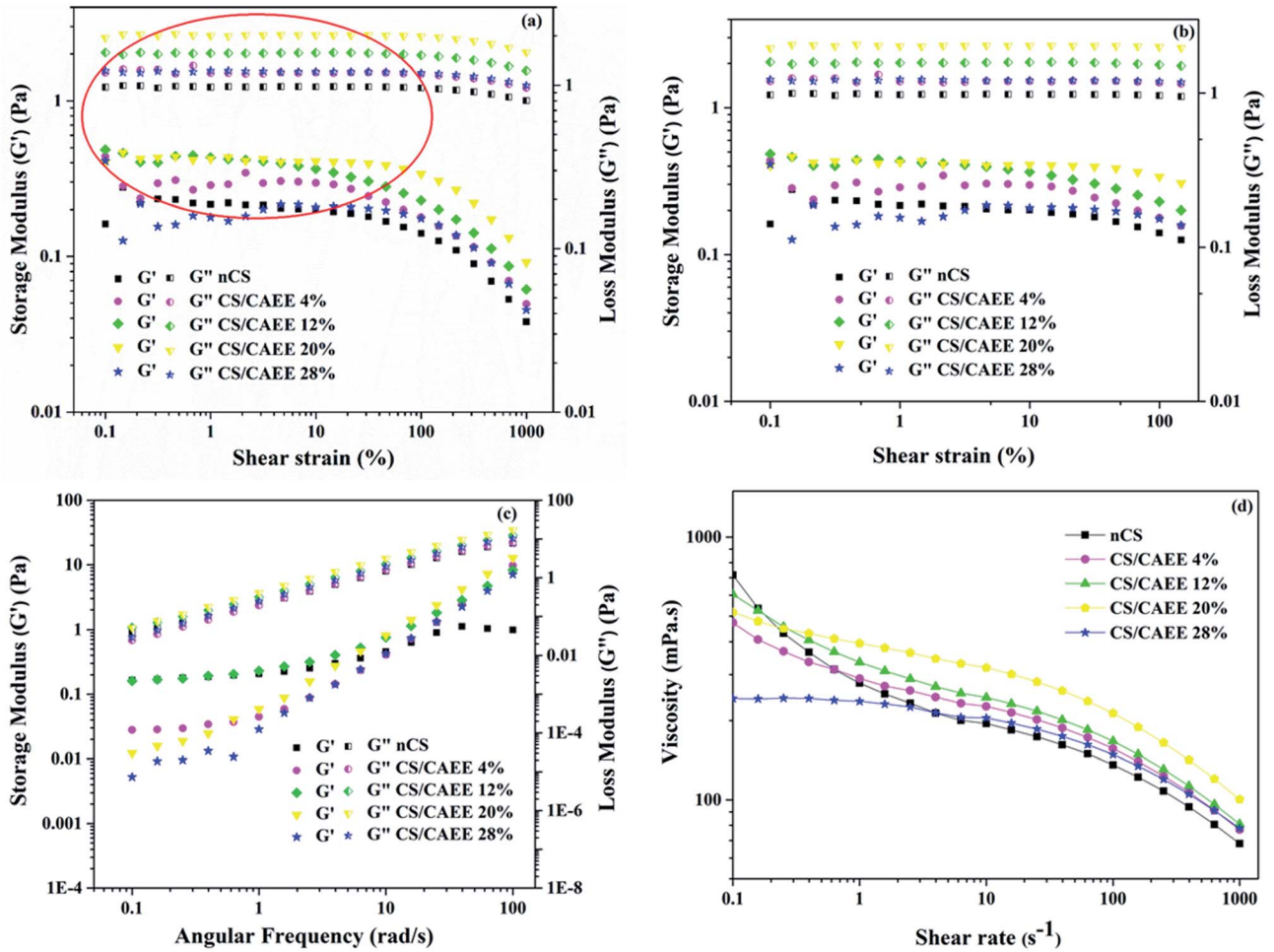

Fig. 8 (a) Strain sweep parameters of the G' and G'' moduli at $f = 1$ Hz, (b) emphasizing the LVR, (c) frequency sweep parameters of the G' and G'' moduli, and (d) flow curves of the developed biocomposite films together with the control.

an impact on slowing down the diffusion rate of water molecules due to the crosslinking, which would have led to a reduction in chain mobility, thereby minimizing the WVP through the film surface.[43] This observed result was corroborated by the FTIR analysis, which also postulated the interaction between the CS matrix and CAEE could be attributed to the shortage of free hydrophilic moieties, including amino and hydroxyl groups, to bind with water, thereby minimizing the water vapor diffusion rate.[44]

Mechanical properties of the developed films. The consequence of incorporating CAEE into the CS-polymer matrix on the mechanical behavior of the CS/CAEE biocomposite edible films was investigated with regard to the tensile strength (TS) and elongation at break (% E). The obtained stress–strain curves of the edible films are shown in Fig. 7c. The increasing trend with the CAEE content was observed with the addition from 4 to 28%, which led to a significant increment in the TS, from 28.62 to 54.1 MPa. Further, a significant increment in the % E of the biocomposites was observed upon the addition of CAEE up till 16% loading, beyond which a slight reduction occurred (Fig. 7d). The improvement in the mechanical property could be related to the uniform and homogeneous distribution of CAEE particles with the CS matrix, which could be responsible for the improved tensile strength. Besides, the reduction in flexibility of the films might be due to the formation of strong hydrogen bonding between the filler and polymer matrix, which could cause a reduction in the chain mobility of the system. However, increasing CAEE concentration beyond 12% led to a slight reduction in both the TS and % E in the resulting CS/CAEE films; however, the values were still higher in comparison to the control. Further, the reduction in mechanical behavior could be attributed to the weak intermolecular interaction between the matrix and filler due to the formation of agglomeration, which provided discontinuities in the polymeric matrix, and allowed the formation of a heterogeneous structure, leading to a loss of cohesion in the developed edible films. A similar type of result has also been reported in the literature, where the addition and increment of the green algae *Ulva armoricana* content from 0 to 30% in a polyvinylalcohol (PVA) matrix did not significantly improve the TS, while a sharp reduction was reported for % E.[45] Chiellini *et al.* (2008) reported reductions in the TS and % E in PVA/algae composite films with

a higher loading of around 30% algae powder in the matrix.[45] They also noted the reduction in the mechanical property might have been caused by the formation of improper crosslinking or bonding between the algae powder and PVA matrix, which might have affected the cohesion property of the developed film.

Rheological behavior

Strain sweep measurements of the developed chitosan-based biocomposite filmogenic solutions. Strain sweep measurements were performed and helped to determine the LVR (linear viscoelastic region) of developed filmogenic solutions, where G' (storage modulus) and G'' (loss modulus) remained constant and independent of the applied strain. This measurement also imparts information regarding the structural strength of a material based on the length of the LVR region, *i.e.*, a stable solution might remain longer in the LVR region as it is more resistant to applied force than an unstable one. The representative curves for the G' and G'' moduli of all the solutions as plotted against the applied strain are depicted in Fig. 8a and b. It is evident from the curve that in all cases $G'' > G'$, indicating that all the samples showed a liquid-like behavior under the LVR.

Overall, the elasticity (G') decreased over time with increasing the shear strain for all the samples, including the control. However, the addition of CAEE significantly improved the elastic behavior compared to the control (nCS), which was more significant at higher strain. Further, a significant increase in G'_{LVR} values with increasing the filler concentration from 4 to 20% was observed; whereas at a higher concentration of CAEE (28%), the G'_{LVR} dropped down, but not below the control value, as described in Table 1, at a fixed shear strain of 1%. Besides, at lower shear strain, a similar trend was visualized for all the samples, except for the higher loading of CAEE (28%), where a slight reduction of G' was observed. Additionally, the non-linearity of the G' and G'' moduli under applied strain indicated the end limit of the LVR region.[9] Moreover, the higher G'' value of the CAEE-incorporated polymeric solution compared to the control solution indicated its viscous nature. The G'' values showed a significant improvement from 0.97 (nCS) to 2.0 (CAEE 20%) Pa with increasing the CAEE concentration from 4 to 28%; however at 28% CAEE addition, G'' decreased sharply, but it was still higher than the control. One of the important parameters of oscillatory rheology is the loss factor or loss tangent ($\tan\delta = G''/G'$), which indicates the characteristics of the material; whereby $\tan\delta > 1$ indicates a viscous nature of the sample as $G'' > G'$, while the sample is elastic when $\tan\delta < 1$ ($G' > G''$), and the sample is in an intermediate phase of a highly concentrated polymer solution and a real gel when $\tan\delta > 0.1$, but where the sample is not a true gel.[46] The $\tan\delta$ value of all the filmogenic solutions in the present study was greater than 1, which predicted a concentrated and viscous nature of the polymeric solution. The incorporation of CAEE into the polymeric matrix decreased the $\tan\delta$ value for the 4% and 12% CAEE (4.14 and 3.61) with increasing the filler loading compared to the control (4.49), which was expected as the addition of these specified concentrations of CAEE improved the elasticity of the CS-based filmogenic solution. However, while the addition of 20% and 28% CAEE significantly increased the $\tan\delta$ value, the G'_{LVR} value was significantly lower at this higher concentration (28%). The discussed parameters from the sweep strain measurements, supported by the G''–G' values at a specified shear strain of 1%, showed that the incorporation of CAEE increased the viscous property of the biocomposite filmogenic solutions. The strain sweep measurements showed the influence of the added filler CAEE on the rheological properties of the chitosan-based biocomposite solutions. The observed significant effects might be correlated to the major interaction between the phenolics groups of CAEE and the cationic groups (NH_3^+) of chitosan *via* hydrogen, covalent, and hydrophobic bonding. The effects were even more with increasing the biofiller content up to 20%. In some studies, no great effects on the rheological behavior were found after the addition of extracts like grape seed, and jabuticaba peel extract in the polymeric matrix due to the use of a small range of extracts.[47] However, other studies showed the influence of the incorporated extract on the rheological properties of the chitosan matrix,[46] like the results obtained from the present study.

Table 1 Strain sweep parameters measured at room temperature with $f = 1$ Hz: critical strain (γ_L), G' modulus at the LVR limit (G'_{LVR}), G'' modulus at the LVR limit (G''_{LVR}), loss factor value ($\tan\delta$) and the difference between G'' and G' moduli at 1% strain

Sample	γ_L (%)	G'_{LVR} (Pa)	G''_{LVR} (Pa)	$\tan\delta$	$G''-G'$ (Pa)	Power-law model (n)	R^2
nCS	31.6	0.21	0.97	4.49	0.75	0.32	0.996
CS/CAEE 4%	46.4	0.28	1.18	4.14	0.90	0.31	0.991
CS/CAEE 12%	68.1	0.43	1.56	3.61	1.13	0.37	0.990
CS/CAEE 20%	99.9	0.42	2.00	4.72	1.58	0.40	0.996
CS/CAEE 28%	147	0.17	1.22	6.88	1.05	0.23	0.994

Frequency sweep measurements of the developed chitosan-based biocomposite filmogenic solutions. While the strain sweep measurements give information about the structural stability of the solutions against an applied deformation, the frequency sweep tests classify the samples as a gel, concentrated, or dilute solution, depending on the storage and loss moduli behavior over the frequency range. If $G' > G''$ is true all over the frequency range, the samples are classified as gels. For samples with $G'' > G'$ at higher frequency, the storage and loss moduli are closer to each other, and it is classified as a dilute solution; if $G'' > G'$ and the moduli intersect inside the frequency range, the solution is considered to be concentrated. From the frequency sweep curve (Fig. 8c), it could be clearly observed that all the samples could be considered as diluted polymer solutions, as already described in the strain sweep tests by the $\tan\delta$ values ($\tan\delta > 1$) (see Table 2). The crossover frequency parameters, obtained from frequency sweep curves,

are listed in Table 2. Between the nCS and CS/CAEE 4%, a shift in the crossover frequency ($\omega_{crossover}$) was observed from 1 to 63.1 rad s^{-1} and an increased value of $G'_{crossover}$ from 0.207 to 7.367 was also observed. No crossover point was noticed for the CS/CAEE 20% and CS/CAEE 28% samples.

Steady shear flow properties of the developed chitosan-based biocomposite filmogenic solutions. The flow curve of the formulated nCS and CAEE-incorporated developed biocomposite filmogenic solutions is depicted in Fig. 8d, with the viscosity of each filmogenic solution shown with respect to the shear rate at room temperature. A non-Newtonian pseudoplastic (shear thinning) behavior was obtained in the control (nCS) as well as in the CAEE-incorporated biocomposites and as a result, the viscosity values decreased with increasing the shear rate. This type of behavior could occur in the case of polymeric solutions. The occurrence of the pseudoplastic behavior was due to the alignment or orientation of polymeric molecules toward the direction of flow where the apparent viscosity decreases under increasing the shear rate, which leads to the formation of a higher order alignment of the polymeric chain toward the applied stress.

Further, the incorporation of CAEE reduced the viscosity in the biocomposites compared to in nCS from 717.66 to 242.98 mPa s (Fig. 8d). The obtained results indicated that the addition of CAEE weakened the intramolecular polymeric bonds of chitosan and acetic acid. The overall viscosity was decreased with increasing the CAEE concentration; however, an improvement in viscosity was noticed in the case of the 12% and 20% loadings as compared to the 4% CAEE. However, this increment was overcome by the significant reduction of the viscosity with the highest CAEE (28%) concentration as compared to the control. As mentioned earlier, CAEE contains various phenolic compounds, such as carotenoids, pheophytin, chlorophyll, β-carotene, and astaxanthin, which loosen the bond interaction among the polymeric chains, as polyphenols are rich in hydroxyl groups (–OH), which could create space between the polymeric chains, thereby increasing the mobility of the chains by providing free space.[48] In this context, similar observations of a reduction in viscosity with the addition of polyphenols, such as pomegranate seed extract,[9] grape seed extract,[46] mutra leaf extract,[48] apple skin,[49] and green tea extract,[50] into CS-based film-forming solutions have been reported in the literature. Besides, the flow behavior index (n) obtained by plotting the viscosity as a function of the shear rate and using the power-law model indicates a pseudoplastic behavior when 'n' is between 0 to 1, with values beyond 1 following a Newtonian behavior.[9] The 'n' values in this study ranged from 0.32–0.40 as shown in Table 1, indicating the pseudoplastic behavior of all the filmogenic solutions, which was corroborated by the observed steady flow behavior. Further, the increase in CAEE concentration in the polymeric solution led to increasing 'n' values, except at higher concentrations (28%), where a slight reduction was noticed. However, the addition of CAEE did not alter the pseudoplastic behavior of the filmogenic solutions.

Table 2 Frequency sweep parameters measured at room temperature for the angular frequency ($\omega_{crossover}$) and storage modulus ($G'_{crossover}$) at the crossover point

Sample	$\omega_{crossover}$ (rad s^{-1})	$G'_{crossover}$ (Pa)
nCS	1	0.207
CS/CAEE 4%	63.1	7.367
CS/CAEE 12%	0.6	0.205
CS/CAEE 20%	—	—
CS/CAEE 28%	—	—

Antioxidant activity and total phenolic content of the developed films. One of the common methods for the determination of antioxidant activity is DPPH free radicals scavenging activity, where DPPH acts as a reducing agent or electron donor. The deep violet color of DPPH radicals is converted to transparent color in the presence of antioxidants, and the absorbance is recorded at 517 nm to calculate the percentage of DPPH antioxidant activity.[51] Fig. 9a depicts the percentage of free radical-scavenging activity and/or antioxidant activity of the CAEE-incorporated biocomposite films. The control film exhibited a moderate scavenging activity of ~21.01%. However, a remarkable improvement in DPPH antioxidant activity was observed in the developed edible CS/CAEE edible films. The DPPH radical-scavenging activity of the biocomposite films increased gradually to 28.81%, 31.85%, 33.86%, 36.92%, 40.16%, 44.21%, and 48.23% with the increasing concentration of CAEE from 4 to 28%, respectively. The rise in antioxidant activity could be attributed to the presence of phenolic compounds and a small fraction of $–CH_2–$ groups in CAEE.[52] However, the biocomposites provided preferable antioxidant properties, indicating the presence of CAEE phenolic hydroxyl groups in the film. The presence of polyphenols in CAEE was previously confirmed by MALDI-TOF-MS and NMR analysis, and the available adequate DPPH free radical-scavenging activity of CAEE (~40%) supported the results for the antioxidant activity of the edible films. Therefore, this analysis exhibited that the addition of CAEE enhanced the antioxidant property of the CS-polymer, significantly. Similar findings of an improvement in antioxidant activity after the incorporation of fruit extract, seed oil in CS-based edible film have been reported in the literature.[52,53]

The total phenolic content (TPC) of the CS/CAEE biocomposite films was determined by the Folin–Ciocalteu phenol reagent method. The TPCs of the films are shown in Fig. 9b. The control film exhibited a TPC of 97.96 μg gallic acid/g film. Moreover, an increasing TPC was observed in the biocomposite with increasing the CAEE loading. The highest TPC obtained in the biocomposites was 423.50 μg gallic acid/g film, which was ~38 times greater than that of the control. Therefore, it can be postulated that the presence of phenolic compounds was responsible for the desirable DPPH antioxidant activity in the films and which showed an increasing trend with enhancing the biofiller (CAEE) concentration, corroborating the results obtained for the DPPH antioxidant activity.[54]

Antimicrobial activity of the formulated active edible coating solution. The antibacterial activity against Gram-negative *E. coli* and Gram-positive *S. aureus* was individually tested for each formulation of CS-based CAEE-incorporated edible coating

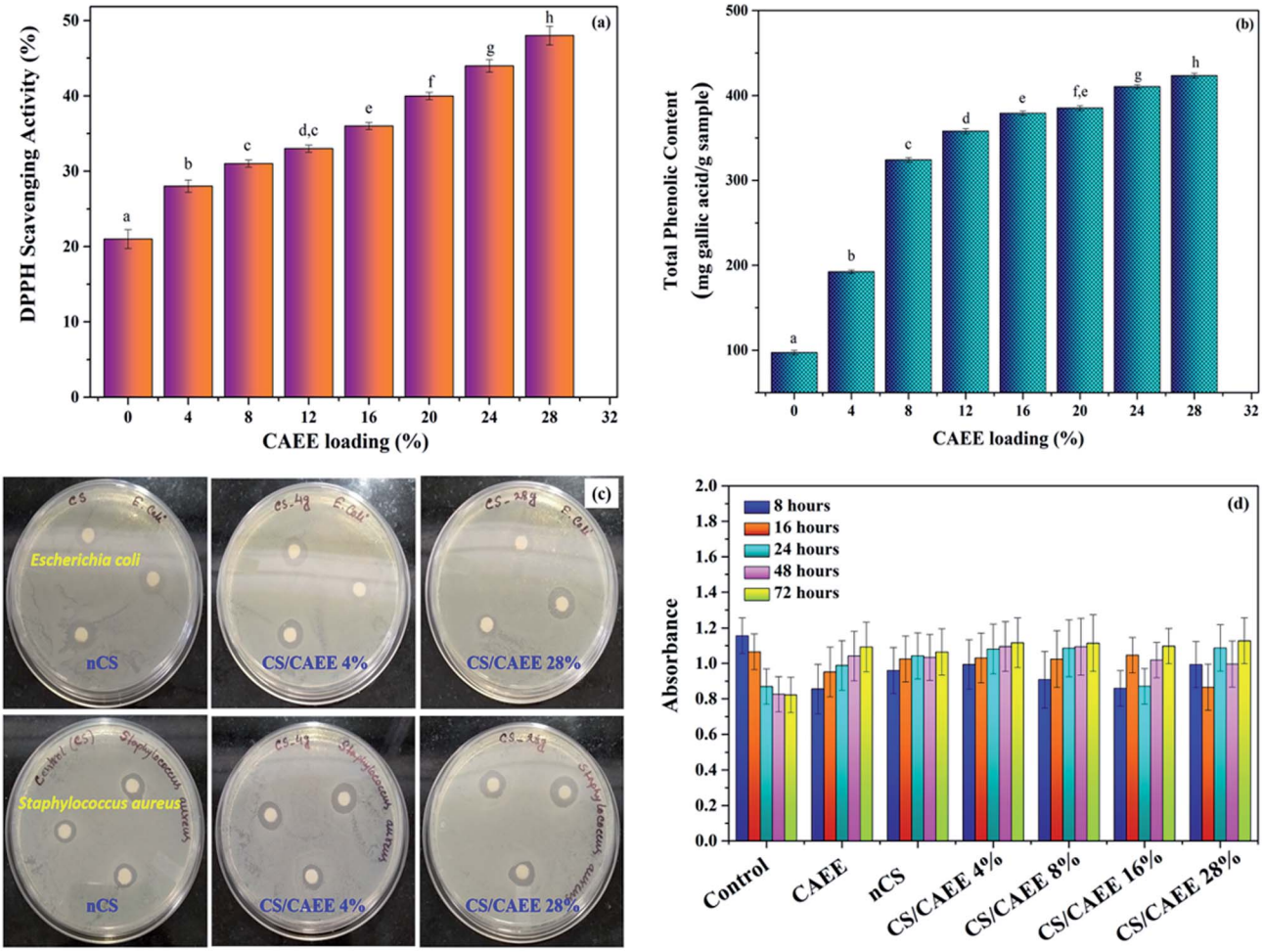

Fig. 9 (a) Antioxidant activity, (b) total phenolic content, (c) antimicrobial activity, and (d) biocompatibility (MTT assay) of the developed biocomposite films compared with the control.

solution, with the solution applied directly on a real food system (green chilli) as a coating. The antimicrobial activity was evaluated using the disk diffusion zone method. The appearance of inhibition zones around the sample confirmed the antimicrobial activity. The accompanying pictures of the tested samples are shown in Fig. 9c. All the filmogenic solutions along with nCS showed clearly visible inhibition zones against both food-borne pathogens. However, a slight increment in the inhibition zone diameter was observed in the biocomposites in comparison to the control neat chitosan solution (Table SI†). The initial concentration of *E. Coli* was 2×10^9 cfu mL^{-1} and S. *aureus* was 4.5×10^9 cfu mL^{-1}.

Biocompatibility of the formulated active coating solution. The cell viability of the developed coating solutions was assessed by MTT assay and the results are depicted in Fig. 9d. The obtained results showed the proliferation of BHK-21 cells over all the filmogenic biocomposite/coating solutions (nCS, CS/CAEE 4%, CS/CAEE 8%, CS/CAEE 16%, CS/CAEE 28%) as well as on CAEE up till 72 h incubation; whereas, a decreasing trend of cell viability was found in the case of the control without the filmogenic solution. This assay suggested the formulated biocomposites/coating solutions were biocompatible and no adverse effect was observed at the end of the study for both the biofiller (CAEE) and coating solutions, respectively, which indicated the formulated coatings could be considered as nontoxic materials and could be explored in the field of edible packaging. The representative images of BHK-21 cells adhered on to the filmogenic solutions and CAEE after 72 h incubation under a bright-field microscope are visualized in SI† together with the control, indicating the biocompatible nature of the formulated edible coating solutions and biofiller.

Coating efficiency effect on the physiological characteristics of green chilli

Weight loss. Weight loss is one of the important parameters for detection of freshness in fresh produce and indicates a deterioration in freshness, with a resulting weight loss ranging between 3–10%.[55] The evaporation of moisture from fresh produce is the reason for the occurrence of shrinkage on the surface of produce. Biopolymer-based films and coatings, such as starch, CS, and alginate, have exhibited significant improvements in retarding the weight loss in fresh produce.[56–58]

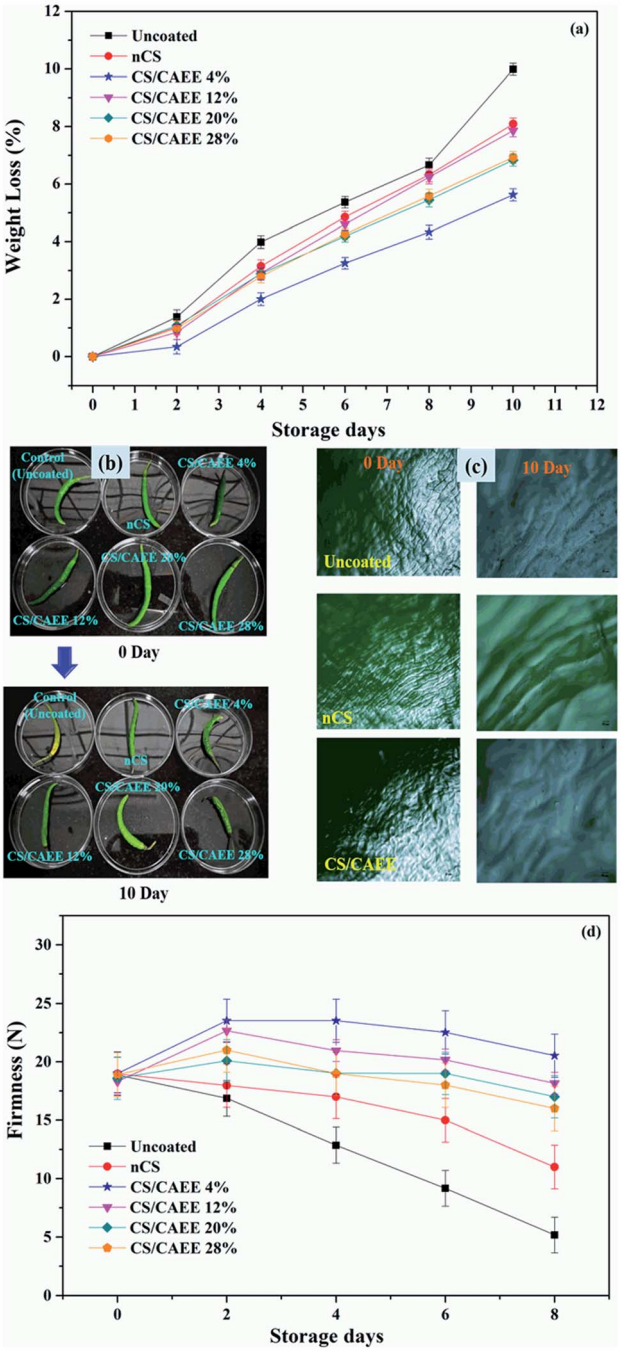

Fig. 10 (a) Physiological weight loss, (b) visual observation, (c) polarized optical microscopic observation, and (d) firmness of stored coated and control green chilli during ambient storage.

A minimal weight loss (WL) was obtained here from the coated green chillies, which were able to maintain a fresh appearance after 7 days of storage under ambient conditions in comparison to the control (uncoated) (Fig. 10a). The difference in weight loss in the coated and control samples was significant ($p < 0.05$). The highest loss of weight of ~9% ($p < 0.05$) was observed in the control samples as compared to the coated chillies, which was showed a weight loss the range of 5–6%. Importantly, the loss percentage was less in the biocomposites compared to nCS coating as well as the control. Therefore, this result indicated that the incorporation of CAEE improved the water vapor barrier property of real food systems, which corroborated the described WVP of the developed CS/CAEE active edible films. The reduction in weight loss in the biocomposites might be due to the strong interaction between the biofiller and polymer matrix as discussed earlier. The minimum WL ($p < 0.05$) was found in the 4% CAEE-added biocomposite film. However, the increasing weight loss during storage could be attributed to *trans*-evaporation and respiration, which are parts of the natural process where the coating could effectively minimize the rate of loss. Basically, during the respiration process, a carbon molecule is usually lost from fruits and causes a weight reduction.[59] Moreover, similar types of results were reported by Xing *et al.* (2011) in the case of bell peppers.[60]

Color parameters and the microstructure. Another characteristic feature of fruit ripening or maturity is the color change, besides the weight loss. During the ripening of chilli fruits, the synthesis of carotenoid pigments occurs (capsanthin and capsorubin are exclusive to this genus in this study).[61] This process is accompanied by a sharp decrease in chlorophyll as a consequence of the degeneration of chloroplast into chromoplast. Respiration of the chillies causes fruit ripening. The coated chillies showed minute changes in color values (L^*, a^*, and b^*), indicating a delay in respiration and senescence, and thereby prolonging the shelf life, as shown in Table SI.† Generally, the coating treatment suppressed the change of green discoloration by partially inhibiting chlorophyll degradation during storage, which could be confirmed from the observation of lower a^* values in the chillies (Table SI†). The coated and control samples showed an increasing trend of L^* and b^* values with the progress of senescence during storage, whereas the coated samples exhibited a slower increment rate. However, the change in color during storage in the chillies also depended on the maturation, presence of carotenoids content, species, composition, and other factors.[62] The coating formulation incorporated with CAEE exhibited a remarkable retention in the color parameter compared to the control and nCS-coated sample, which suggested the addition of CAEE tailored the physicochemical properties of the CS matrix by building strong intermolecular hydrogen bonding between the hydroxyl groups of the active molecules of CAEE with the polymer matrix. In this context, similar observations have been reported on a variety of peppers.[59,60] The visual appearances of the coated green chillies along with the uncoated ones are depicted in Fig. 10b.

It is crystal clear that the control sample exhibited surface dryness and a wilting effect during storage under ambient conditions, whereas the coated samples appeared to be fresh. However, a higher concentration of CAEE (28%) was less effective compared to a lower concentration, which might be due to the agglomeration of CAEE particles inside the polymer matrix. Further, the microstructure of the stored samples was captured under a polarized optical microscope (POM), where surface roughness was observed in the control compared to the coated samples (Fig. 10c). Although, some particles were also visualized over the CS/CAEE-coated samples due to the addition of CAEE.

Firmness. Reduced firmness in fresh produce signifies an inferior quality of fruits, which is caused due to respiration. In this context, the modified atmosphere at the exterior of the food surfaces exhibited a retention in firmness when exposed to high levels of carbon monoxide.[63] The occurrence of softness in fruits is correlated to mechanical damage, microbial contamination, and moisture loss. In the present study, the measured firmness value dropped for the uncoated and coated chillies with increasing the storage time. However, a very slow reduction was observed in the biocomposites compared to the control and nCS-coated chillies while stored under ambient conditions (Fig. 10d). The optimum result was observed for 4% CAEE loading. In addition, when fresh produce undergoes aerobic respiration during storage, it enables the production of superoxide radicals, which can disturb the cell wall structure and allow pectinase enzyme to access the cell wall polysaccharides, such as pectin, to degrade and causes softness in the produce, thereby reducing the produce post-harvest life.[58] Therefore, a combination of techniques could adequately be used to preserve the firmness of green chillies during post-harvest storage.

Conclusion

The present study involved the successful fabrication of chitosan-based edible active biocomposites incorporated with CAEE as a biofiller as a secondary packaging material and application of a formulated filmogenic solution as a coating material on a real food system (fresh produce). The CAEE was obtained by the ultrasound-assisted sustainable extraction of waste de-oil green algae biomass (*Dunaliella tertiolecta*). The extract, CAEE, was rich in antioxidants and various bioactive compounds, predominantly carotenoids, proteins, and polysaccharides. The properties of the fabricated active edible films with varying CAEE contents were analyzed and compared with the control film. The fabricated edible films displayed a superior antioxidant activity, total phenolic content, water vapor barrier property, thermal stability, and mechanical strength. An excellent UV-Vis light-blocking property was observed in the developed edible active film due to the strong interaction of polyphenols with the polymer matrix. The rheological property of the filmogenic solutions exhibited a stable shear thinning (viscous liquid) behavior. The cell line study suggested the developed coating material was biocompatible and nontoxic. Finally, green chillies were coated with the filmogenic solution as a primary packaging and stored under ambient conditions, and a prolonged shelf life of the coated green chilli was demonstrated compared to the control. Besides, coated chilli packed edible pouches made by the developed edible films as secondary packaging material preserved the chillies for a longer period. The promising outcomes from this study suggest that the fabricated edible films could be used as edible active pouches and at the same time the developed filmogenic solution could also be used as a coating material for extending the shelf life of fresh produce.

Author contributions

Kona Mondal: data curation, formal analysis, investigation, original draft writing, review, and editing. Sayan Bhattacharjee: experimental, and original draft. Chethana Mudenur: experimental. Tabli Ghosh: experimental. Vaibhav V. Goud: supervision, and original draft. Vimal Katiyar: conceptualization; funding acquisition, project administration, resources, supervision, validation, visualization, review, and editing.

Conflicts of interest

The authors declare no conflicts of interest.

Acknowledgements

The authors are sincerely thankful to the Centre of Excellence for Sustainable Polymers (CoE-SusPol), Centre for Sustainable Polymers (CSP), and CIF (Center Instrument Facility) at the Indian Institute of Technology Guwahati (IITG) for providing all the possible research and experimental facilities during this work. We are also thankful to TERI-DBT (The Energy and Resource Institute) CoE on Bio-fuels and Bio-commodities (xCLESPNxDBT00860xxVK010, DBT, GOI) for providing raw materials for this work.

Notes and references

1 S. Remya, C. O. Mohan, J. Bindu, G. K. Sivaraman, G. Venkateshwarlu and C. N. Ravishankar, *J. Food Sci. Technol.*, 2016, **53**, 685–693.
2 U. Siripatrawan and B. R. Harte, *Food Hydrocolloids*, 2010, **24**, 770–775.
3 D. Moreira, B. Gullón, P. Gullón, A. Gomes and F. Tavaria, *Food Funct.*, 2016, **7**, 3273–3282.
4 A. R. Deshmukh, H. Aloui, C. Khomlaem, A. Negi, J. H. Yun, H. S. Kim and B. S. Kim, *Food Chem.*, 2021, **337**, 127777.
5 J. Deng, E. Q. Zhu, G. Xu, N. Naik, V. Murugadoss, M. G. Ma and Z. Shi, *Green Chem.*, 2021, **24**, 480–492.
6 M. S. Nair, A. Saxena and C. Kaur, *Food Bioprocess Technol.*, 2018, **11**, 1317–1327.
7 K. Mondal, T. Ghosh, P. Bhagabati, and V. Katiyar, Sustainable Nanostructured Materials in Food Packaging, *Dynamics of Advanced Sustainable Nanomaterials and their Related Nanocomposites at the Bio-Nano Interface*, Elsevier, 2019, pp. 171–213.
8 P. K. Dutta, S. Tripathi, G. K. Mehrotra and J. Dutta, *Food Chem.*, 2009, **114**, 1173–1182.
9 M. R. Bertolo, V. C. Martins, M. M. Horn, L. B. Brenelli and A. M. Plepis, *Carbohydr. Polym.*, 2020, **228**, 115386.
10 T. Ghosh, Y. Teramoto and V. Katiyar, *J. Agric. Food Chem.*, 2019, **67**, 4289–4299.
11 S. M. Ojagh, M. Rezaei, S. H. Razavi and S. M. H. Hosseini, *Food Chem.*, 2010, **122**, 161–166.
12 F. Nowzari, B. Shábanpour and S. M. Ojagh, *Food Chem.*, 2013, **141**, 1667–1672.
13 T. C. Dos Santos, N. Rescignano, L. Boff, F. H. Reginatto, C. M. O. Simões, A. M. de Campos and C. U. Mijangos, *Carbohydr. Polym.*, 2017, **173**, 638–644.
14 C. O. Ferreira, C. A. Nunes, I. Delgadillo and J. A. Lopes-da-Silva, *Food Res. Int.*, 2009, **42**, 807–813.

15 N. K. Kalita, M. K. Nagar, C. Mudenur, A. Kalamdhad and V. Katiyar, *Polym. Test.*, 2019, **76**, 522–536.
16 W. Lan, R. Zhang, S. Ahmed, W. Qin and Y. Liu, *LWT*, 2019, **113**, 108297.
17 U. Bhardwaj, P. Dhar, A. Kumar and V. Katiyar, *Am. Chem. Soc.*, 2014, 275–314.
18 H. Akretche, G. Pierre, R. Moussaoui, P. Michaud and C. Delattre, *Green Chem.*, 2019, **21**, 3065–3073.
19 W. Zhang, X. Li and W. Jiang, *Int. J. Biol. Macromol.*, 2020, **154**, 1205–1214.
20 A. Silva-Weiss, V. Bifani, M. Ihl, P. J. A. Sobral and M. C. Gómez-Guillén, *Food Hydrocolloids*, 2013, **31**, 458–466.
21 X. Zhang, H. Lian, J. Shi, W. Meng and Y. Peng, *Int. J. Biol. Macromol.*, 2020, **148**, 1242–1250.
22 T. Liu, L. Liu, X. Gong, F. Chi and Z. Ma, *LWT*, 2021, **135**, 110181.
23 J. M. Lorenzo, P. E. Munekata, A. S. Sant'Ana, R. B. Carvalho, F. J. Barba, F. Toldrá and M. A. Trindade, *Trends Food Sci. Technol.*, 2018, **77**, 1–10.
24 S. Zou, Y. Wu, M. Yang, C. Li and J. Tong, *Energy Fuel.*, 2009, **23**, 3753–3758.
25 A. S. Sarpal, C. M. Teixeira, S. Mesquita, I. C. Costa and R. M. S. Paulo, *Adv. Appl. Microbiol.*, 2018, **11**, 555812.
26 A. S. Sarpal, C. M. Teixeira, P. R. M. Silva, T. V. da Costa Monteiro, J. I. da Silva, V. S. da Cunha and R. J. Daroda, *Appl. Microbiol. Biotechnol.*, 2016, **100**, 2471–2485.
27 P. M. Foley, E. S. Beach and J. B. Zimmerman, *Green Chem.*, 2011, **13**, 1399–1405.
28 K. Mondal, S. Sakurai, Y. Okahisa, V. V. Goud and V. Katiyar, *Carbohydr. Polym.*, 2021, **261**, 117881.
29 K. Mondal, P. Bhagabati, V. V. Goud, S. Sakurai and V. Katiyar, *Int. J. Biol. Macromol.*, 2021, **191**, 521–530.
30 A. Hosikian, S. Lim, R. Halim and M. K. Danquah, *Int. J. Chem. Eng.*, 2010, 2010.
31 M. J. Iglesias, R. Soengas, I. Probert, E. Guilloud, P. Gourvil, M. Mehiri and F. L. Ortiz, *Phytochemistry*, 2019, **164**, 192–205.
32 R. Nicolau, M. Leloup, D. Lachassagne, E. Pinault and G. Feuillade-Cathalifaud, *Talanta*, 2015, **136**, 102–107.
33 P. D. Fraser, E. M. Enfissi, M. Goodfellow, T. Eguchi and P. M. Bramley, *Plant J.*, 2007, **49**, 552–564.
34 A. Mishra, K. Kavita and B. Jha, *Carbohydr. Polym.*, 2011, **83**, 852–857.
35 K. Tsukida, K. Saiki and M. Sugiura, *J. Nutr. Sci. Vitaminol.*, 1981, **27**, 551–561.
36 L. Wang, Y. Dong, H. Men, J. Tong and J. Zhou, *Food Hydrocolloids*, 2013, **32**, 35–41.
37 X. Zhang, Y. Liu, H. Yong, Y. Qin, J. Liu and J. Liu, *Food Hydrocolloids*, 2019, **94**, 80–92.
38 H. Yong, X. Wang, R. Bai, Z. Miao, X. Zhang and J. Liu, *Food Hydrocolloids*, 2019, **90**, 216–224.
39 A. R. Deshmukh, J. W. Jeong, S. J. Lee, G. U. Park and B. S. Kim, *ACS Sustainable Chem. Eng.*, 2019, **7**, 17114–17125.
40 A. R. Deshmukh, H. Aloui and B. S. Kim, *J. Cleaner Prod.*, 2020, **270**, 122339.
41 M. Bajić, T. Ročnik, A. Oberlintner, F. Scognamiglio, U. Novak and B. Likozar, *Food Packag. Shelf Life*, 2019, **21**, 100365.
42 S. U. Kadam, S. K. Pankaj, B. K. Tiwari, P. J. Cullen and C. P. O'Donnell, *Food Packag. Shelf Life*, 2015, **6**, 68–74.
43 P. Hernández-Muñoz, A. López-Rubio, J. M. Lagarón and R. Gavara, *Biomacromolecules*, 2004, **5**, 415–421.
44 A. Gupta, A. K. Pal, E. M. Woo and V. Katiyar, *Sci. Rep.*, 2018, **8**, 1–13.
45 E. Chiellini, P. Cinelli, V. I. Ilieva and M. Martera, *Biomacromolecules*, 2008, **9**, 1007–1013.
46 M. Romanelli Vicente Bertolo, V. da Conceicao Amaro Martins, A. M. de GuzziPlepis and S. Bogusz Jr, *J. Appl. Polym. Sci.*, 2021, **138**, 50052.
47 M. Á. V. Rodrigues, M. R. V. Bertolo, C. A. Marangon, V. D. C. A. Martins and A. M. de GuzziPlepis, *Int. J. Biol. Macromol.*, 2020, **160**, 769–779.
48 A. Silva-Weiss, V. Bifani, M. Ihl, P. J. A. Sobral and M. C. Gómez-Guillén, *J. Food Eng.*, 2014, **140**, 28–38.
49 W. X. Du, C. W. Olsen, R. J. Avena-Bustillos, M. Friedman and T. H. McHugh, *J. Food Sci.*, 2011, **76**, M149–M155.
50 Y. Peng, Q. Wang, J. Shi, Y. Chen and X. Zhang, *Food Sci. Technol.*, 2019, **40**, 162–170.
51 M. Kaya, P. Ravikumar, S. Ilk, M. Mujtaba, L. Akyuz, J. Labidi and S. K. Erkul, *Innovative Food Sci. Emerging Technol.*, 2018, **45**, 287–297.
52 K. I. Priyadarsini, D. K. Maity, G. H. Naik, M. S. Kumar, M. K. Unnikrishnan, J. G. Satav and H. Mohan, *Free Radicals Biol. Med.*, 2003, **35**, 475–484.
53 E. Talón, K. T. Trifkovic, V. A. Nedovic, B. M. Bugarski, M. Vargas, A. Chiralt and C. González-Martínez, *Carbohydr. Polym.*, 2017, **157**, 1153–1161.
54 M. Jouki, F. T. Yazdi, S. A. Mortazavi and A. Koocheki, *Food Hydrocolloids*, 2014, **36**, 9–19.
55 S. Ben-Yehoshua, and V. Rodov, Transpiration and Water Stress, *Postharvest Physiology and Pathology of Vegetables*, CRC Press, 2002, pp. 143–197.
56 O. P. Chauhan, C. Nanjappa, N. Ashok, N. Ravi, N. Roopa and P. S. Raju, *J. Food Sci. Technol.*, 2015, **52**, 1200–1205.
57 K. Chitravathi, O. P. Chauhan and P. S. Raju, *Postharvest Biol. Technol.*, 2014, **92**, 146–148.
58 K. Chitravathi, O. P. Chauhan, P. S. Raju and N. Madhukar, *Food Bioprocess Technol.*, 2015, **8**, 1386–1392.
59 K. Chitravathi, O. P. Chauhan and P. S. Raju, *J. Food Sci. Technol.*, 2016, **53**, 3320–3328.
60 Y. Xing, X. Li, Q. Xu, J. Yun, Y. Lu and Y. Tang, *Food Chem.*, 2011, **124**, 1443–1450.
61 M. I. Minguez-Mosquera and D. Hornero-Mendez, *J. Agric. Food Chem.*, 1994, **42**, 1555–1560.
62 R. J. Cogdell, T. D. Howard, R. Bittl, E. Schlodder, I. Geisenheimer and W. Lubitz, *Philos. Trans. R. Soc. London, Ser. B*, 2000, **355**, 1345–1349.
63 P. S. Tanada-Palmu and R. F. G. Carlos, *Postharvest Biol. Technol.*, 2005, **36.2**, 199–208.
64 K. Godlewska, I. Michalak, Ł. Tuhy and K. Chojnacka, *BioMed Res. Int.*, 2017, **2017**, 7248634.

65 S. Dudonné, P. Poupard, P. Coutiere, M. Woillez, T. Richard, J. M. Mérillon and X. Vitrac, *J. Agric. Food Chem.*, 2011, **59**, 4527–4536.
66 C. M. Bitencourt, C. S. Fávaro-Trindade, P. D. A. Sobral and R. A. Carvalho, *Food Hydrocolloids*, 2014, **40**, 145–152.
67 Y. Fang, M. A. Tung, I. J. Britt, S. Yada and D. G. Dalgleish, *J. Food Sci.*, 2002, **67**, 188–193.
68 N. Limchoowong, P. Sricharoen, S. Techawongstien and S. Chanthai, *Food Chem.*, 2016, **200**, 223–229.